Finanziato dall'Unione europea NextGenerationEU
Ministero dell'Università e della Ricerca
Italiadomani PIANO NAZIONALE DI RIPRESA E RESILIENZA
Dipartimento di Fisica e Astronomia
UNIVERSITÀ DEGLI STUDI DI PADOVA
Agenzia Spaziale Italiana Explorer

magnetar sources

Roberto Taverna (speaker)
Roberto Turolla, Silvia Zane, Jeremy Heyl, Fabio Muleri, Luca Baldini, Matteo Bachetti, Ilaria Caiazzo, Niccolò Di Lalla, Alessandro Di Marco, Ephraim Gau, Denis Gonzalez, Gian Luca Israel, Ruth Kelly, Demet Kırmızıbayrak, Henric Krawczynski, Fabio La Monaca, Michela Negro, Mason Ng, Nicola Omodei, Andrea Possenti, John Rankin, Toru Tamagawa, Keisuke Uchiyama, Martin C. Weisskopf
and the IXPE team

International X-ray Polarimetry Symposium (IXPO)
Strongly Magnetized Neutron Stars
Huntsville, September 16–19, 2024

Magnetars

- Anomalous X-ray Pulsars – Soft γ-repeaters
- X-ray luminosity (usually) in excess of the $\dot{E}_{\rm rot}$
- Isolated
- $P = 1 - 12$ s
  $\dot{P} = 10^{-13} - 10^{-9}$ s/s $\Rightarrow$ $B_{\rm sd} = 10^{14} - 10^{15}$ G

$\Downarrow$

Magnetars !

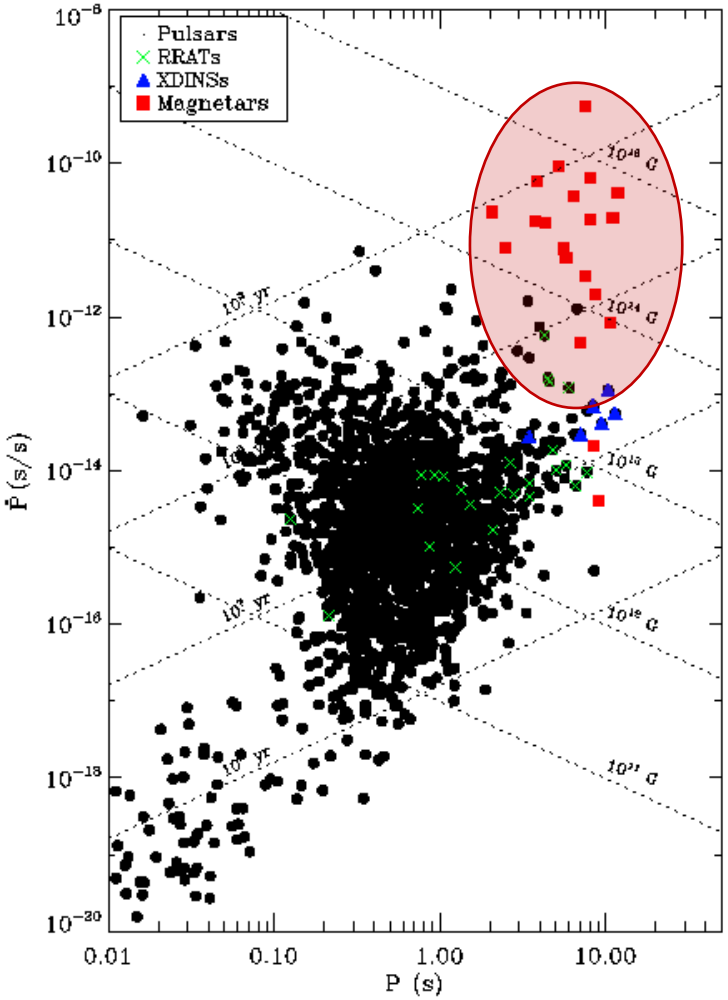

Persistent and transient sources

Persistent sources

- $L_{\rm X} = 10^{33} - 10^{36}$ erg/s
- Soft X-ray spectra: BB+PL / BB+BB
  $kT_{\rm BB} \approx 0.5 - 1.0$ keV
  $\Gamma \approx 2 - 4$

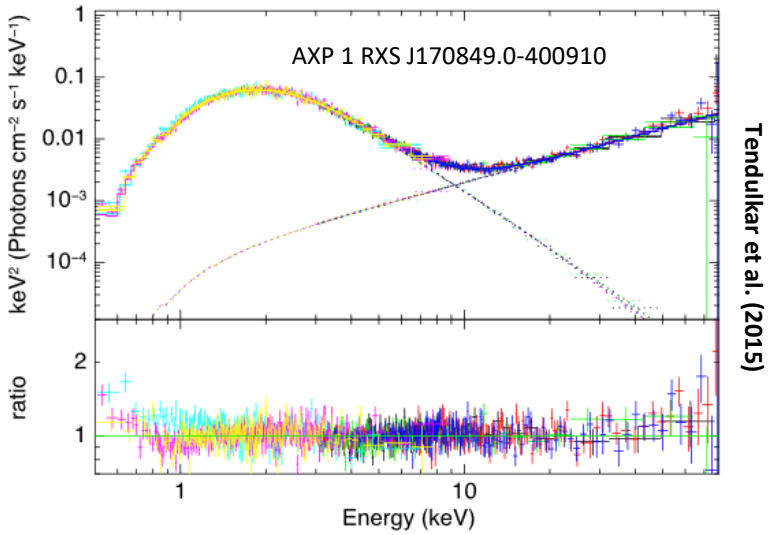

Tendulkar et al. (2015)

Transients

- $L_{\rm X} = 10^{31} - 10^{35}$ erg/s
- Sudden enhancement of flux $(100 - 1000\times)$ for $\approx 10 - 10^3$ days (outbursts)
- Essentially thermal spectra (BB+BB)

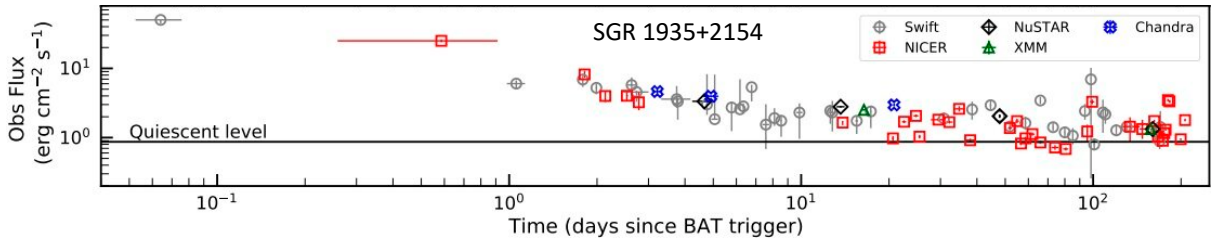

Borghese et al. (2022)

Burst and flare emission

Bursting activity (≠ outbursts)

- Occurrence of bursts/flares, observed in both persistent and transient sources (especially during outbursts)
- Three types of events
  - Short bursts
  - Intermediate flares
  - Giant flares

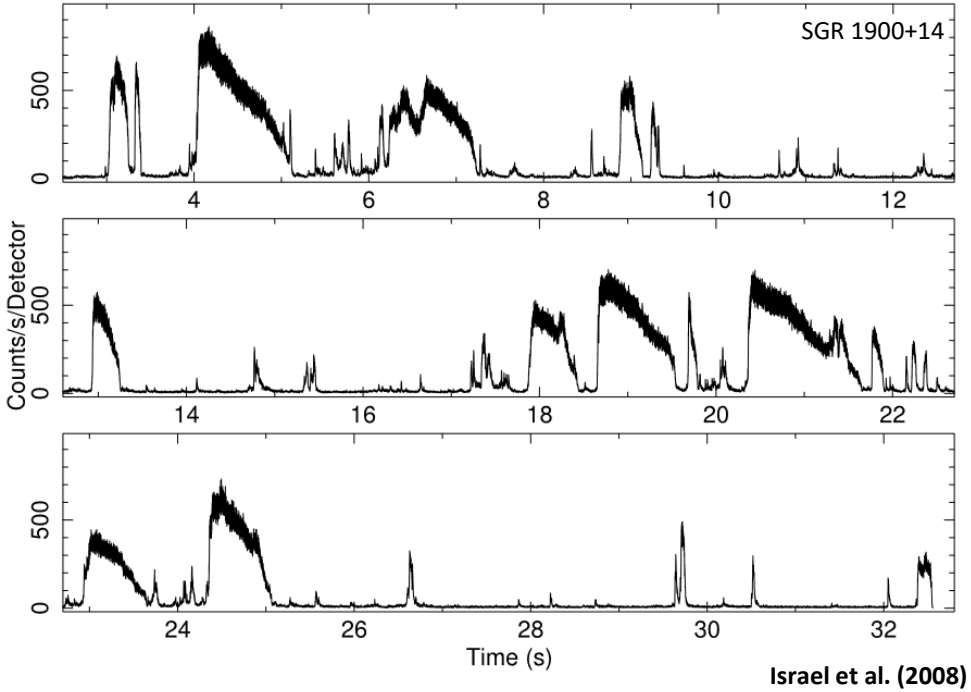

Israel et al. (2008)

Magnetar model – Twisted-magnetosphere

- The strong internal field (up to 10^{16} G) should develop a toroidal component at least of the same order

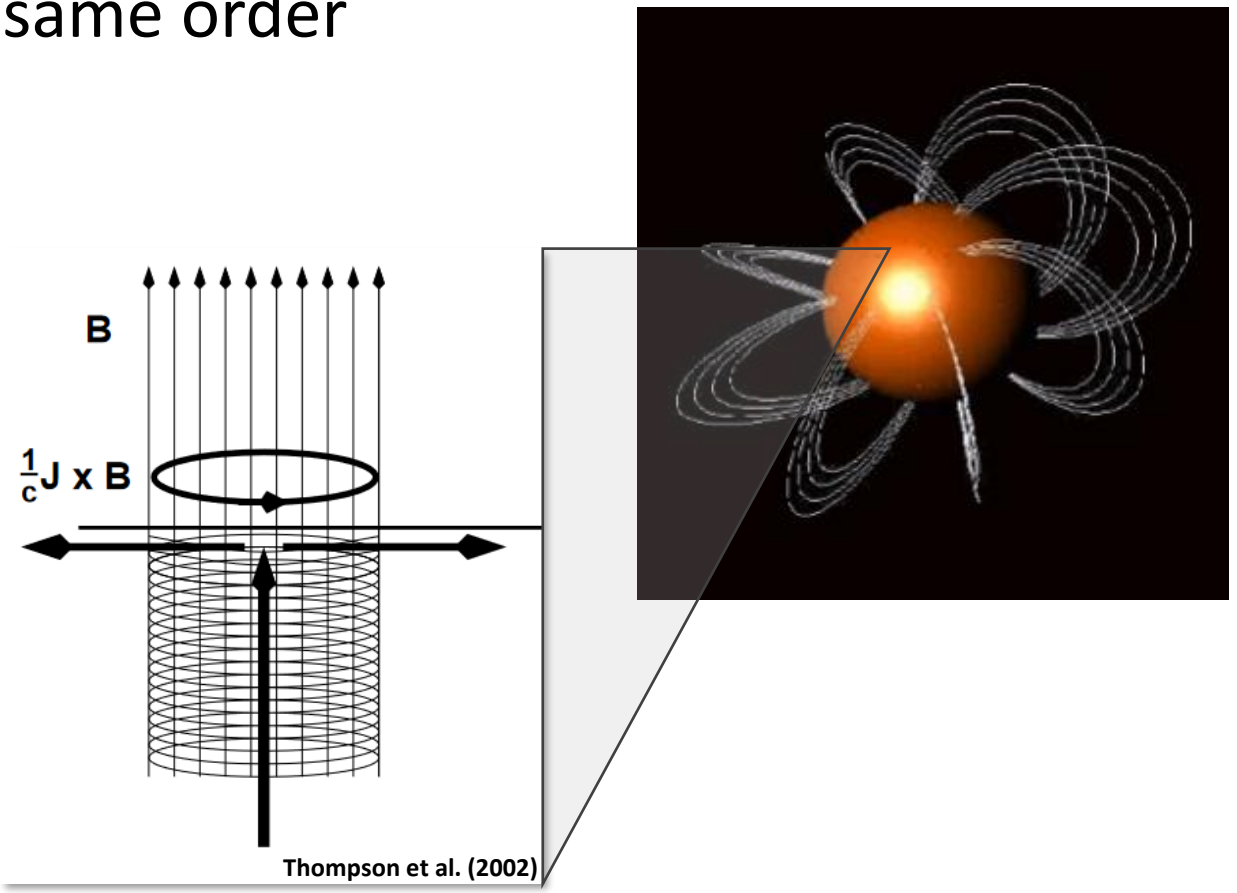

Magnetar model – Twisted-magnetosphere

- The strong internal field (up to 10^{16} G) should develop a toroidal component at least of the same order
- Once the magnetic stress exceeds the crust mechanical yield, helicity is transferred to the external field

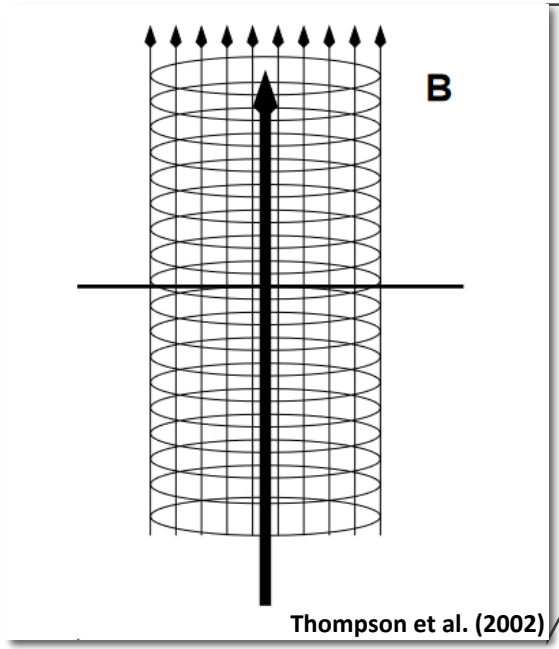

Thompson et al. (2002)

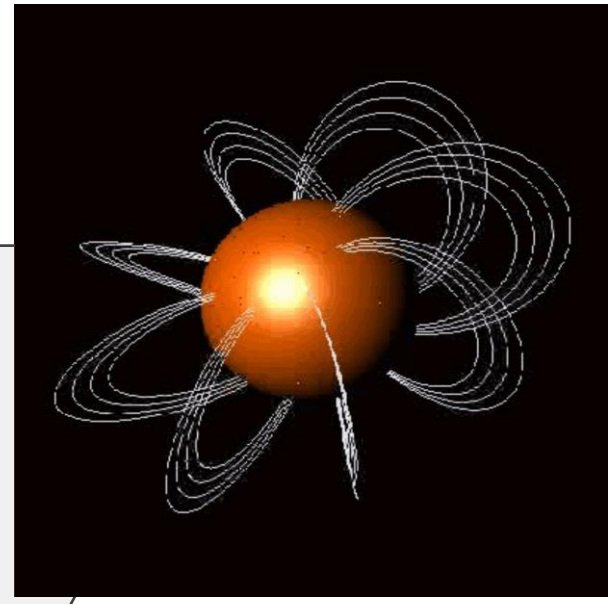

Magnetar model – Twisted-magnetosphere

- The strong internal field (up to 10^{16} G) should develop a toroidal component at least of the same order
- Once the magnetic stress exceeds the crust mechanical yield, helicity is transferred to the external field
- Non-potential field ⇒ currents must flow along close field lines
- Magnetosphere is optically thick for Resonant Compton Scattering RCS

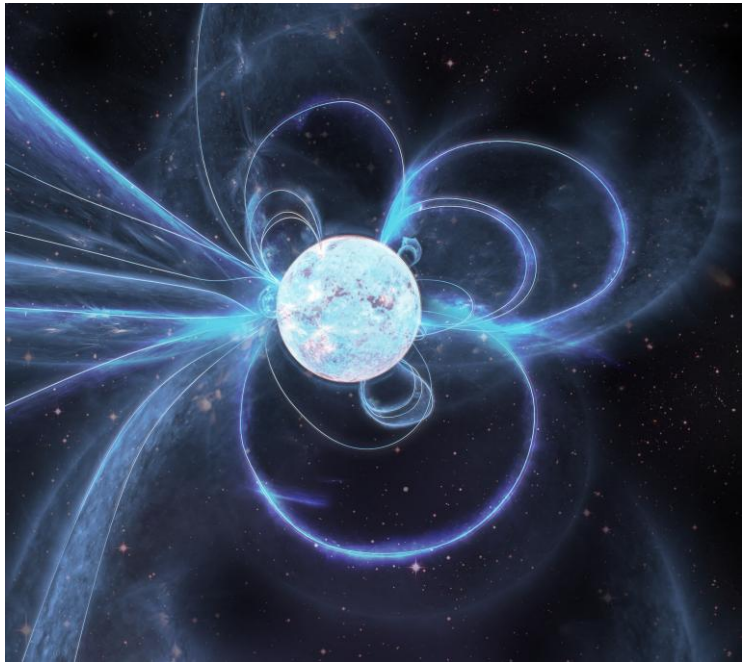

Magnetar model – Implications

- RCS of thermal photons onto magnetospheric particles generates PL tails at soft X-ray energies

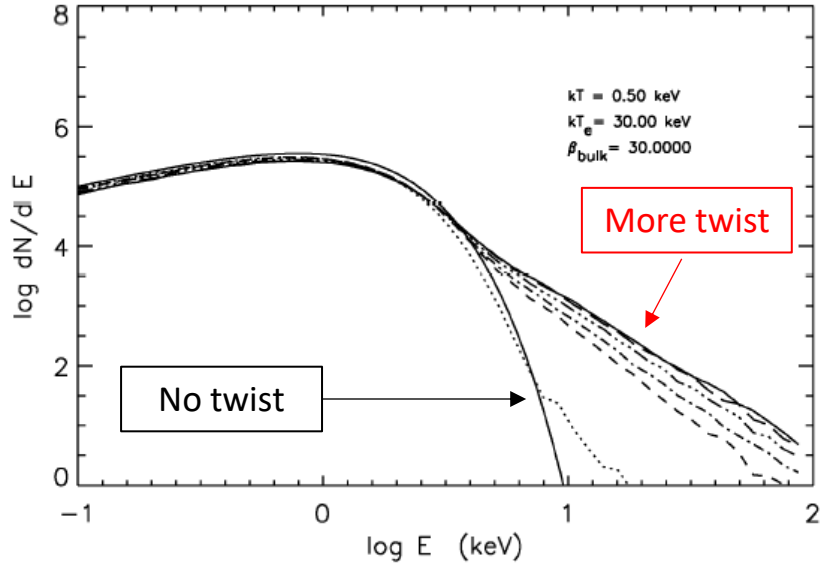

Nobili et al. (2008)

Magnetar model – Implications

- RCS of thermal photons onto magnetospheric particles generates PL tails at soft X-ray energies
- Local B-field structure may form ⇒ returning currents may heat isolated spots on the surface

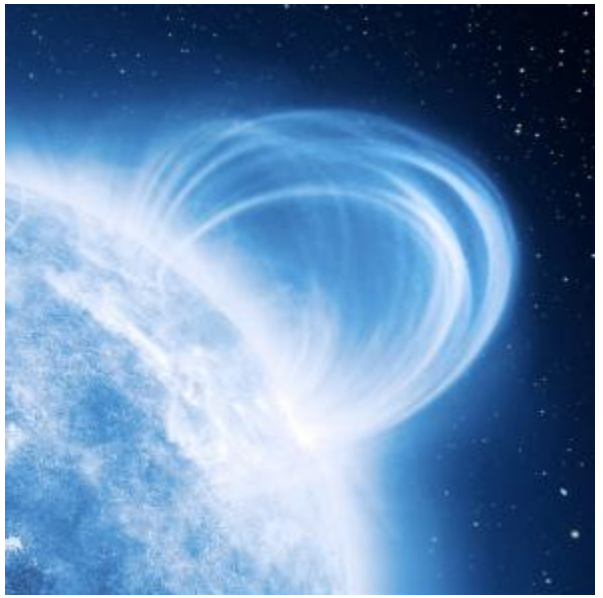

Credit: ESA Science & Technology

Magnetar model – Implications

- RCS of thermal photons onto magnetospheric particles generates PL tails at soft X-ray energies
- Local B-field structure may form ⇒ returning currents may heat isolated spots on the surface
- Injection of $e^- e^+$ fireballs in the magnetosphere induced by crust deformations (at the base of burst/flare emission)

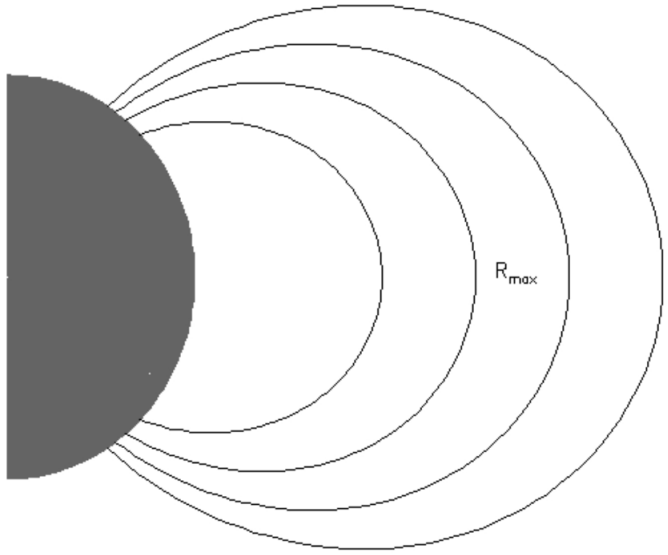

Are magnetars really NSs?

- The P-$\dot{P}$ estimate of the magnetic field strength holds for:
  - dipolar fields (magnetar field topology not dipolar)
  - emission energy all supplied by rotation (not valid for magnetars)
- Alternative models
  - strongly-magnetized ($\approx 10^9$ G) white dwarfs (e.g. 2020ApJ...895...26B)
  - manifestations of some kind of explosion (e.g. 1999A&AS—138..507F)
- Hard to put a clear constraint with timing and spectroscopy alone
- Polarimetry helps!

Polarization in strong B-fields

- The polarization state of photons can be studied solving the wave equation

$$\boldsymbol{\nabla} \times (\bar{\boldsymbol{\mu}} \cdot \boldsymbol{\nabla} \times \boldsymbol{E}) = \frac{\omega^2}{c^2} \boldsymbol{\epsilon} \cdot \boldsymbol{E}$$

magnetic permeability tensor (inverse)

dielectric tensor

Polarization in strong B-fields

- The polarization state of photons can be studied solving the wave equation

$$\boldsymbol{\nabla} \times (\bar{\boldsymbol{\mu}} \cdot \boldsymbol{\nabla} \times \boldsymbol{E}) = \frac{\omega^2}{c^2} \boldsymbol{\epsilon} \cdot \boldsymbol{E}$$

- $\boldsymbol{\epsilon}$ and $\bar{\boldsymbol{\mu}}$ contain:

Plasma terms

- Collisions
- Coulomb interactions
- Radiation damping

Vacuum terms

- Vacuum polarization – magnetized virtual $e^- e^+$ make vacuum behaving as a birefringent medium (for $B \gtrsim B_Q \approx 4 \times 10^{13}$ G)

Normal modes of polarization

- For ultra strong B-fields ($\gtrsim B_Q$) photons at X-ray energies are linearly polarized in two normal modes

$$\widehat{\boldsymbol{E}} \approx \begin{pmatrix} 1 \\ 0 \\ 0 \end{pmatrix} \quad \text{or} \quad \begin{pmatrix} 0 \\ 1 \\ 0 \end{pmatrix}$$

Ordinary mode **Extraordinary mode**

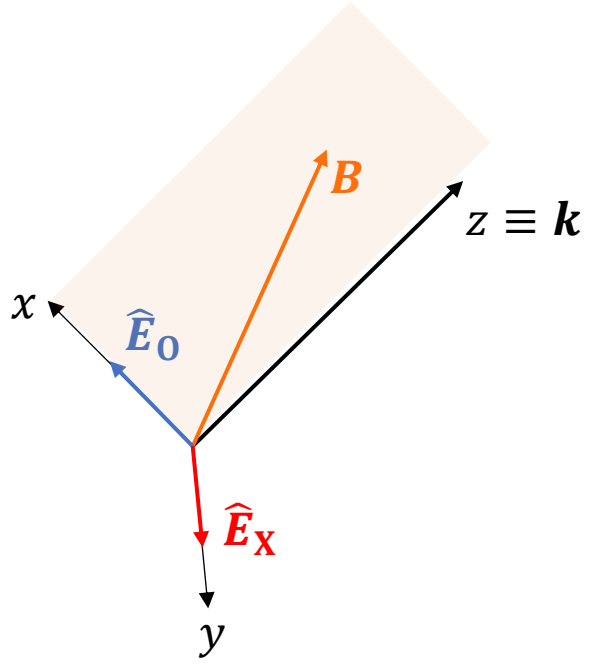

Normal modes of polarization

- For ultra strong B-fields ($\gtrsim B_Q$) photons at X-ray energies are linearly polarized in two normal modes
- Polarization evolution depends on the density of material in which photons propagate

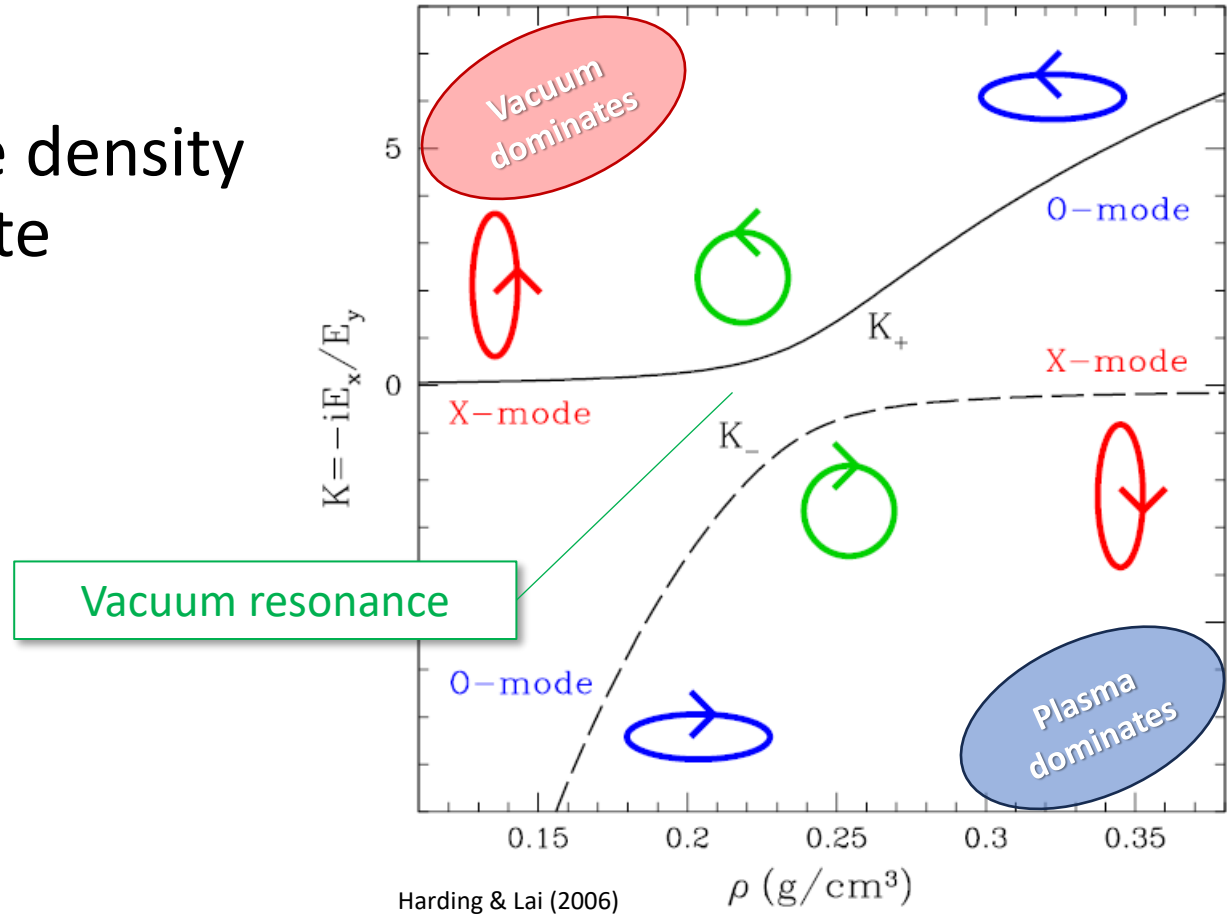

Harding & Lai (2006)

Dichroism in strongly-magnetized plasma

- In strong fields ($B \gtrsim B_{\rm Q}$) and $E \ll \hbar\omega_B$ plasma is (generally) transparent for X-mode photons

$$\sigma_{\rm OO} \sim \sigma_{\rm unmag} \qquad \sigma_{\rm XO} \sim \left(\frac{B}{B_Q}\right)^{-2} \sigma_{\rm OO}$$

$$\sigma_{\rm OX} \sim \left(\frac{B}{B_{\rm Q}}\right)^{-2} \sigma_{\rm OO} \qquad \sigma_{\rm XX} \sim \left(\frac{B}{B_{\rm Q}}\right)^{-2} \sigma_{\rm OO}$$

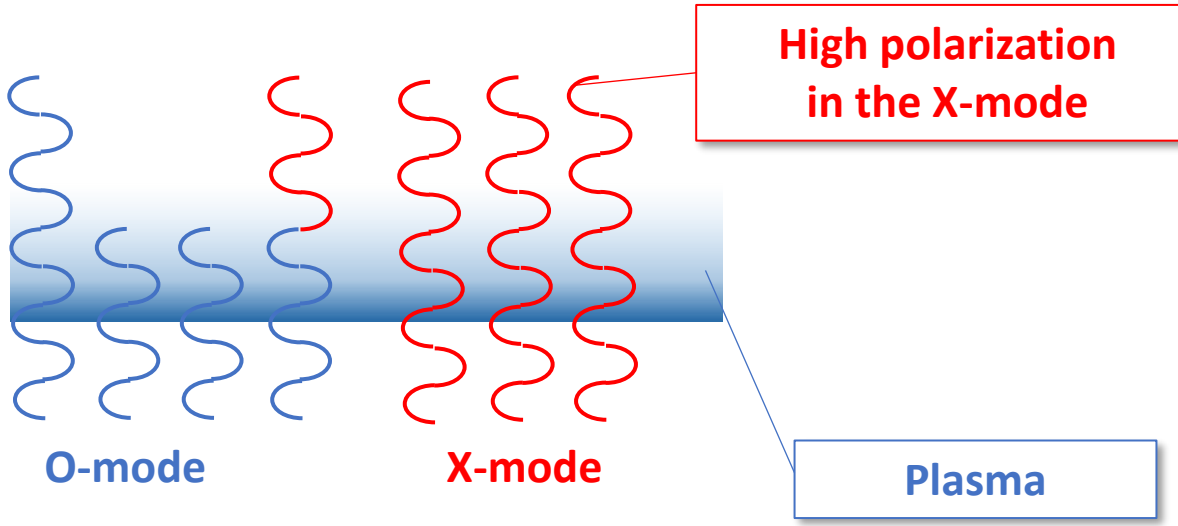

Dichroism in strongly-magnetized plasma

- In strong fields ($B \gtrsim B_{\rm Q}$) and $E \ll \hbar\omega_B$ plasma is (generally) transparent for X-mode photons
- Things are different at the cyclotron resonance ($\omega = \omega_{\rm B}$)

$$\sigma_{\rm OO} = \frac{1}{3}\sigma_{\rm Ox}$$

larger probability to emerge in the X-mode

$$\sigma_{\rm XX} = 3\sigma_{\rm XO}$$

larger probability to emerge in the X-mode

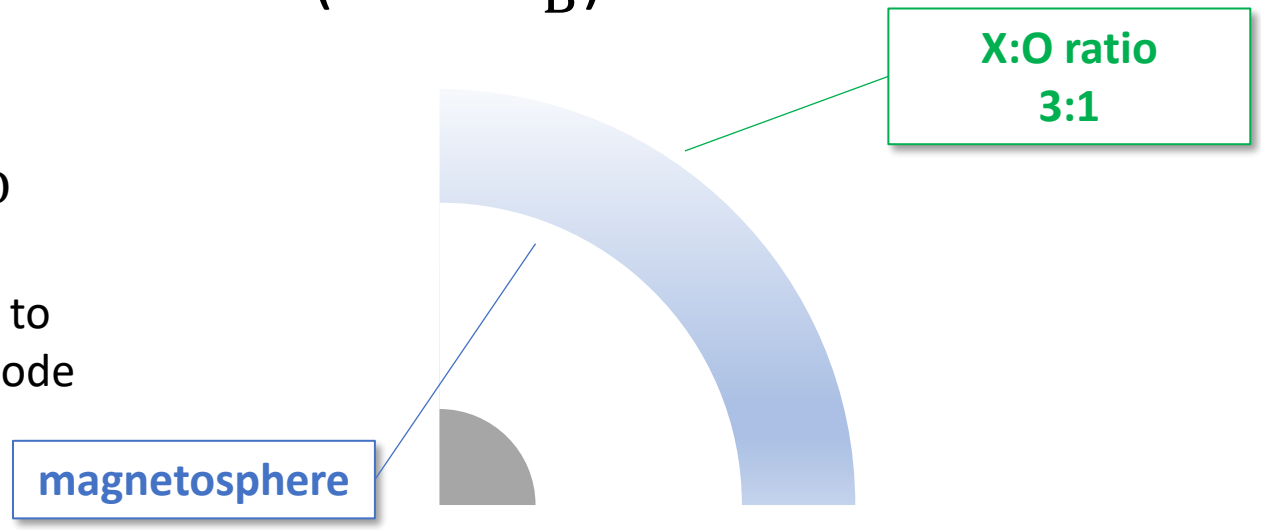

Polarization transport in the magnetized vacuum

- Solving the wave equation accounting for vacuum effects only it reduces to

$$\frac{2}{k_0\delta(B)}\frac{dE_x}{dz} = i\left[ME_x + PE_y\right] \qquad \frac{2}{k_0\delta(B)}\frac{dE_y}{dz} = i\left[PE_x + NE_y\right]$$

Polarization transport in the magnetized vacuum

- Solving the wave equation accounting for vacuum effects only it reduces to

$$\frac{2}{k_0\delta(B)}\frac{dE_x}{dz} = i\left[ME_x + PE_y\right] \qquad \frac{2}{k_0\delta(B)}\frac{dE_y}{dz} = i\left[PE_x + NE_y\right]$$

E-field evolution length:

$$\ell_{\rm E} = \frac{2}{k_0\delta} \approx 130\left(\frac{B}{10^{11}\ {\rm G}}\right)^{-2}\left(\frac{\hbar\omega}{1\ {\rm keV}}\right)^{-1}\ {\rm cm}$$

(Dipolar) B-field evolution length:

$$\ell_{\rm B} = \frac{B}{|\boldsymbol{k}\cdot\boldsymbol{\nabla}B|} \approx \frac{r}{3}$$

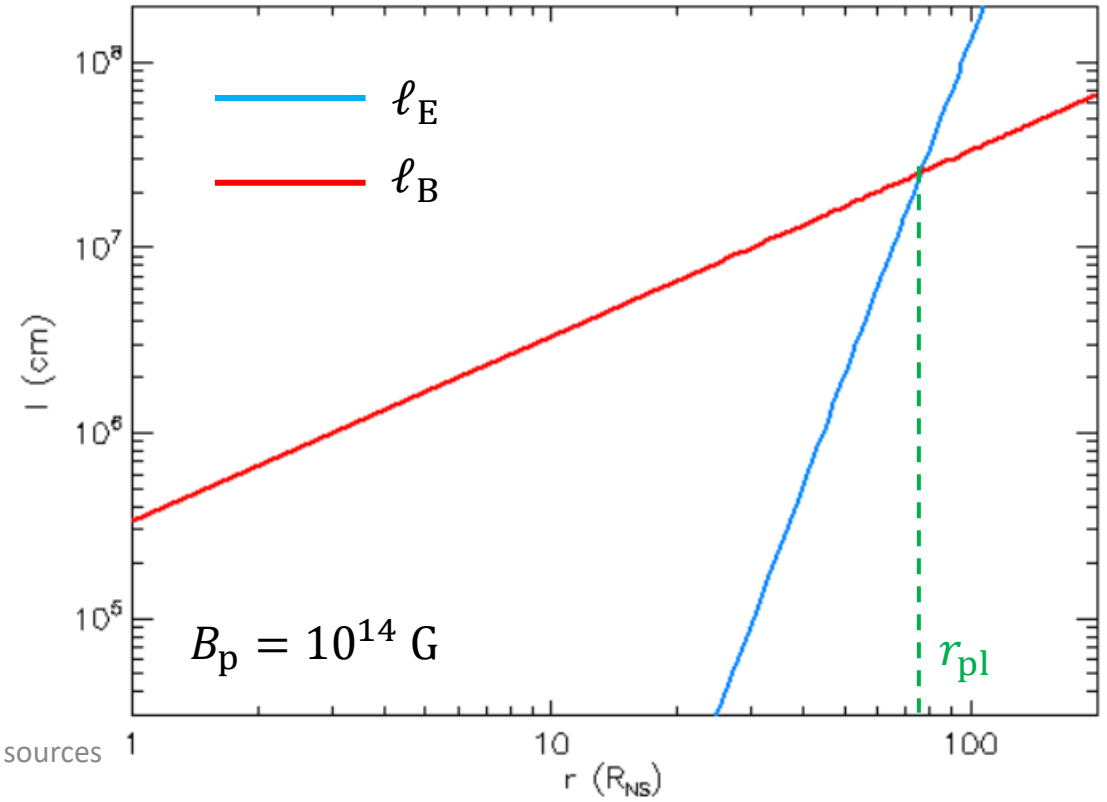

Polarization transport in the magnetized vacuum

- Solving the wave equation accounting for vacuum effects only it reduces to

$$\frac{2}{k_0\delta(B)}\frac{dE_x}{dz} = i\left[ME_x + PE_y\right] \qquad \frac{2}{k_0\delta(B)}\frac{dE_y}{dz} = i\left[PE_x + NE_y\right]$$

$\ell_{\mathrm{E}} \gg \ell_{\mathrm{B}}$: $\boldsymbol{E}$ direction is frozen

r_{pl} $(\ell_{\mathrm{E}} = \ell_{\mathrm{B}})$

$\ell_{\mathrm{E}} \ll \ell_{\mathrm{B}}$: $\boldsymbol{E}$ adapts to $\boldsymbol{B}$

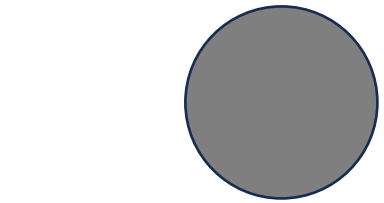

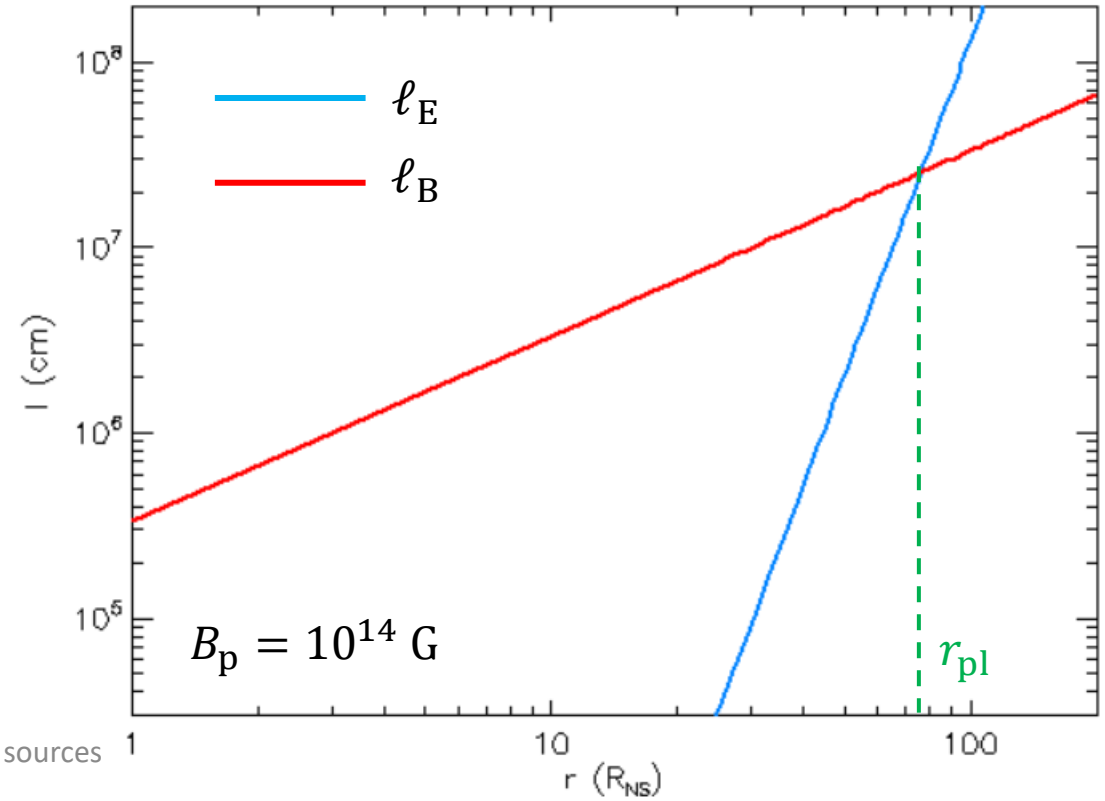

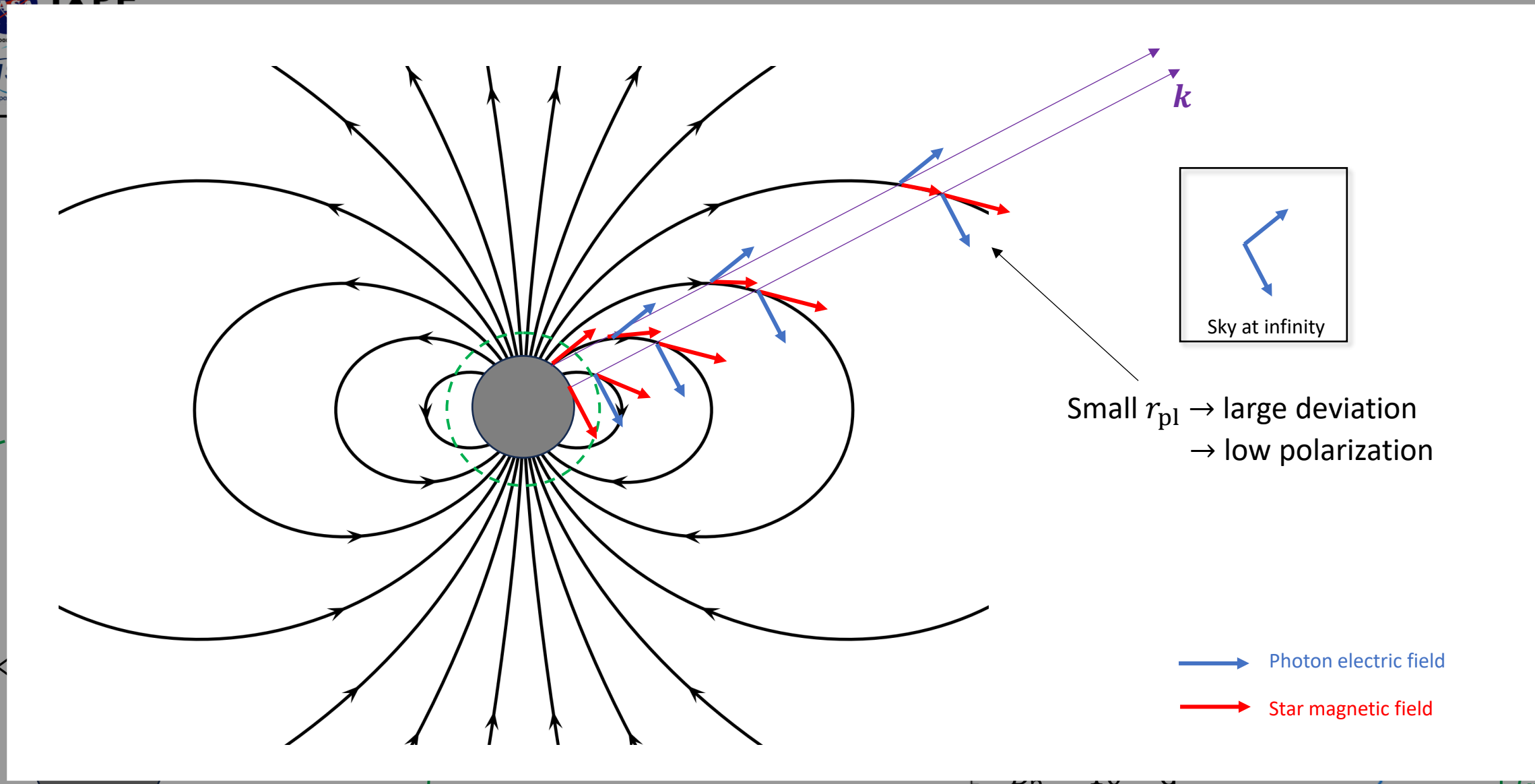
k
Sky at infinity
Small $r_{\rm pl}$ → large deviation
→ low polarization
Photon electric field
Star magnetic field

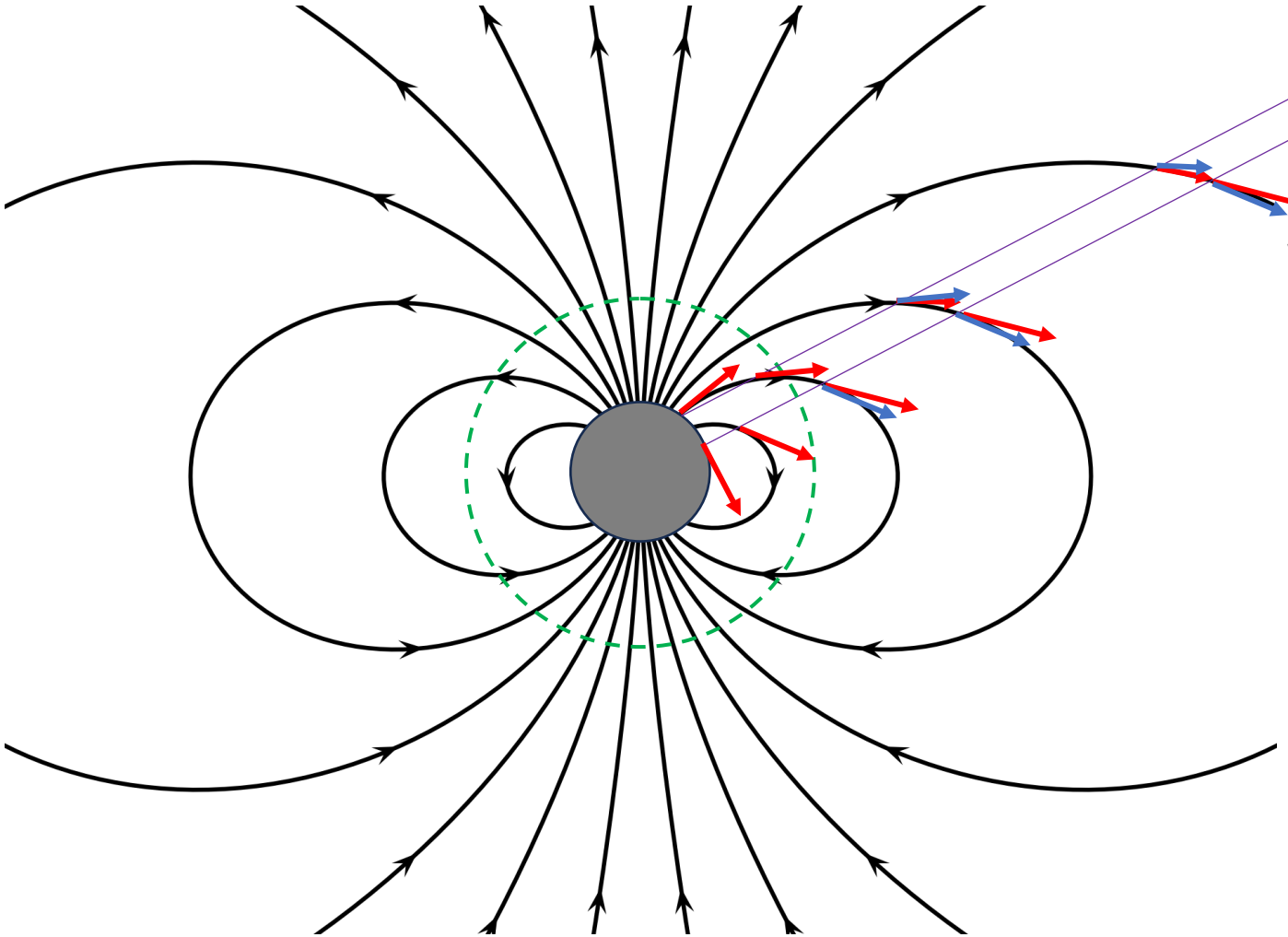

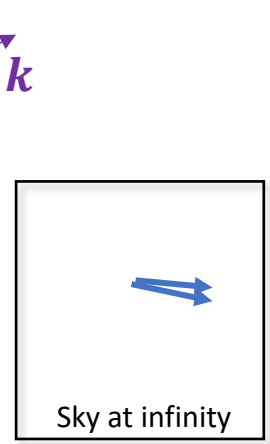

Large $r_{\rm pl}$ → small deviation
→ high polarization

Photon electric field

Star magnetic field

$\ell_{\rm E}$ <

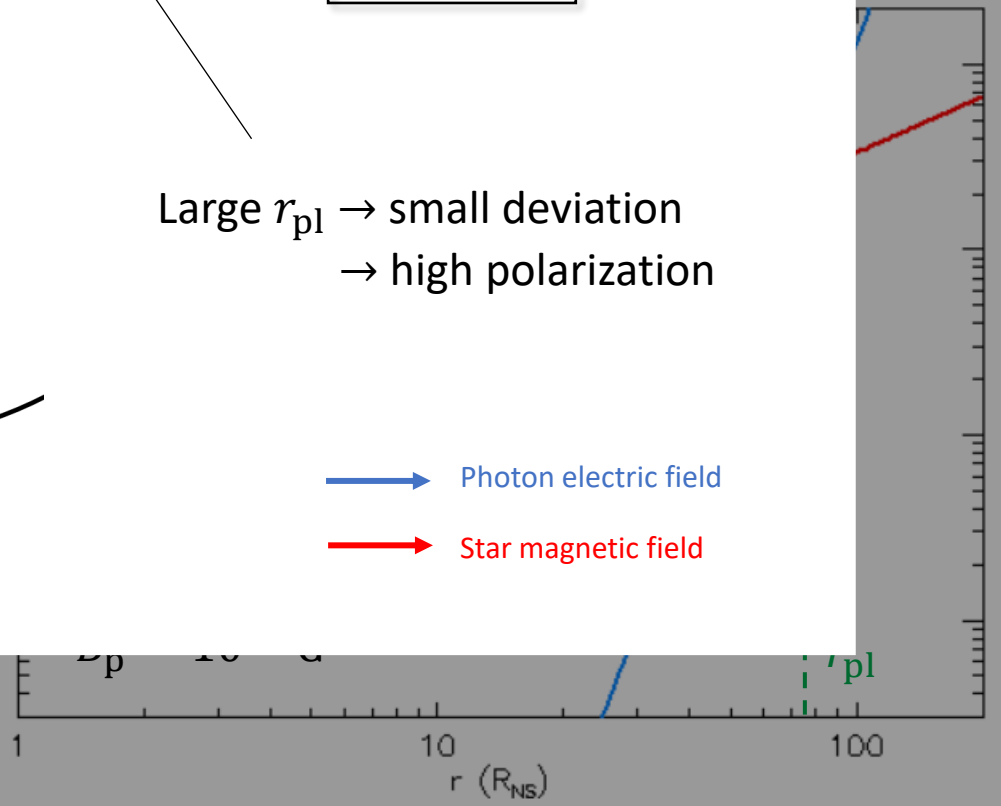

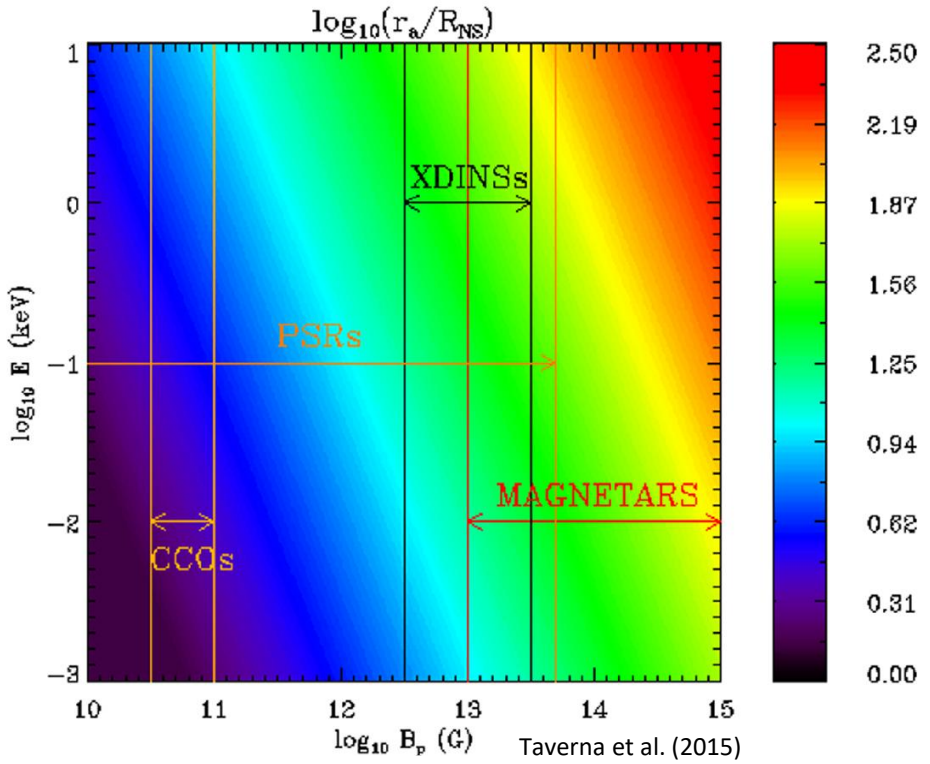

Taverna et al. (2015)

Magnetars (with the strongest $\boldsymbol{B}$) have the largest $r_{\rm pl}$

⇓

Best candidates to observe polarization of surface emission (potentially very high)

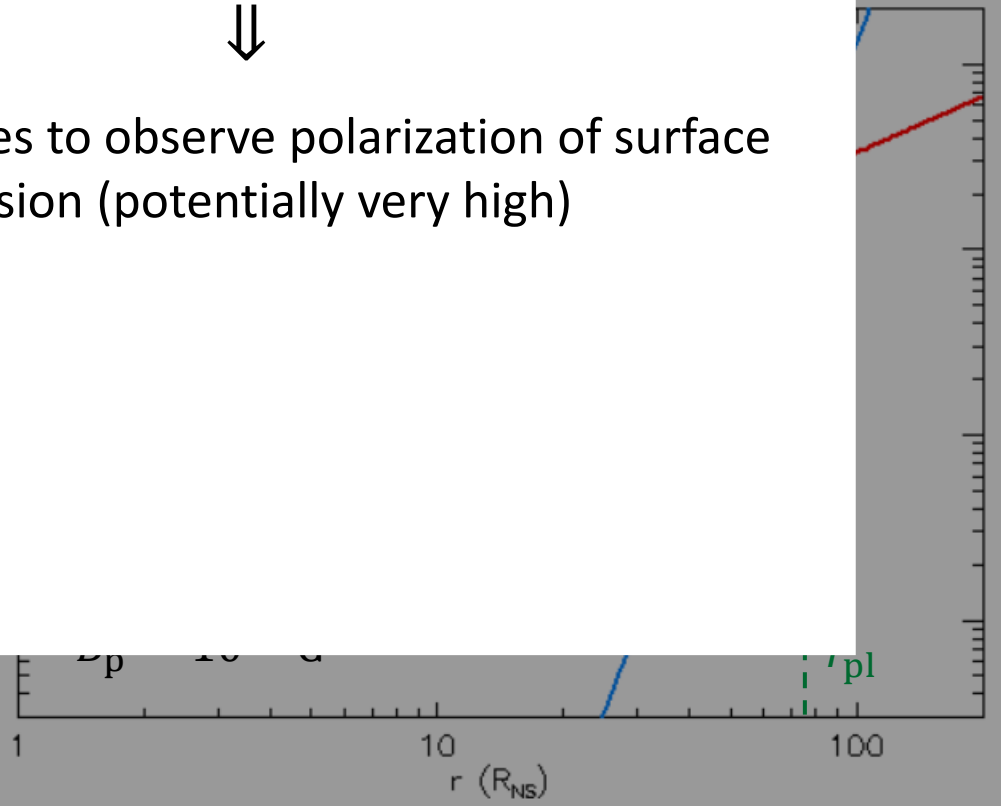

Surface emission models

- Surface photons reprocessed by a standard, magnetized atmosphere → high PD (X-mode)

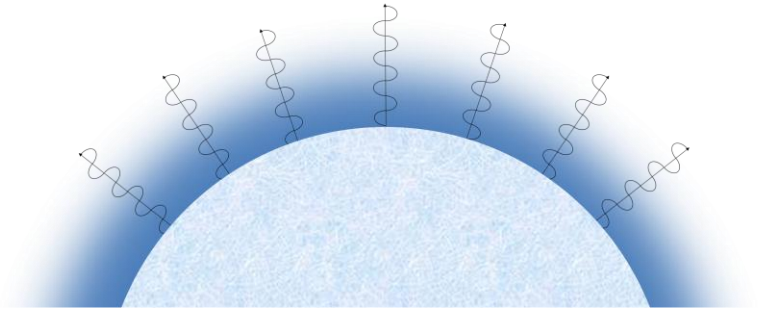

PD ≳ 80%

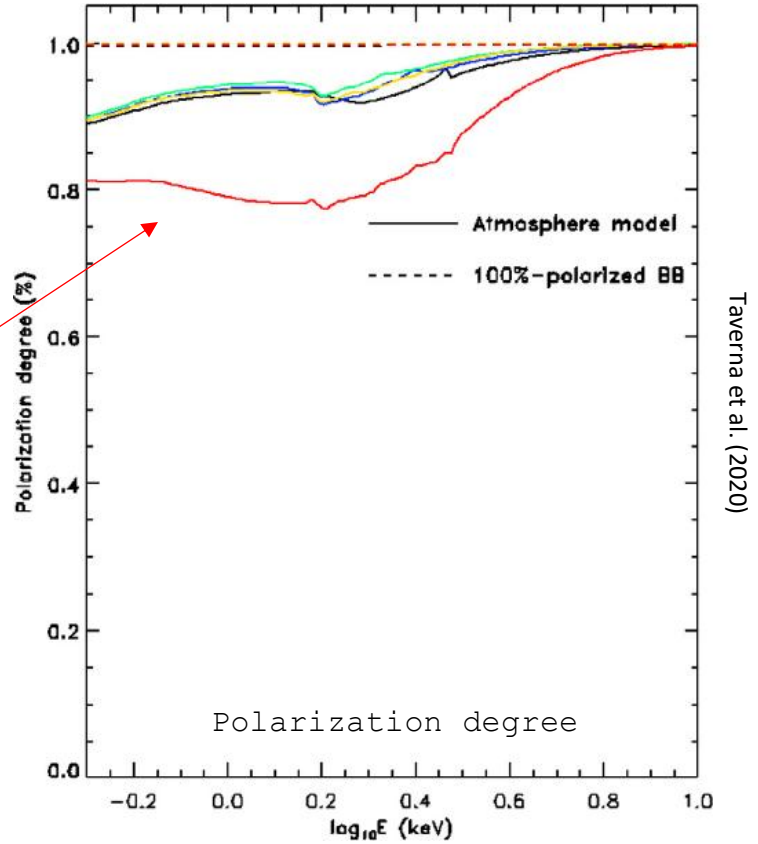

Taverna et al. (2020)

Surface emission models

- Surface photons reprocessed by a standard, magnetized atmosphere → high PD (X-mode)
- Very strong B-fields elongate atoms along the field direction → molecular chains are formed for sufficiently low T

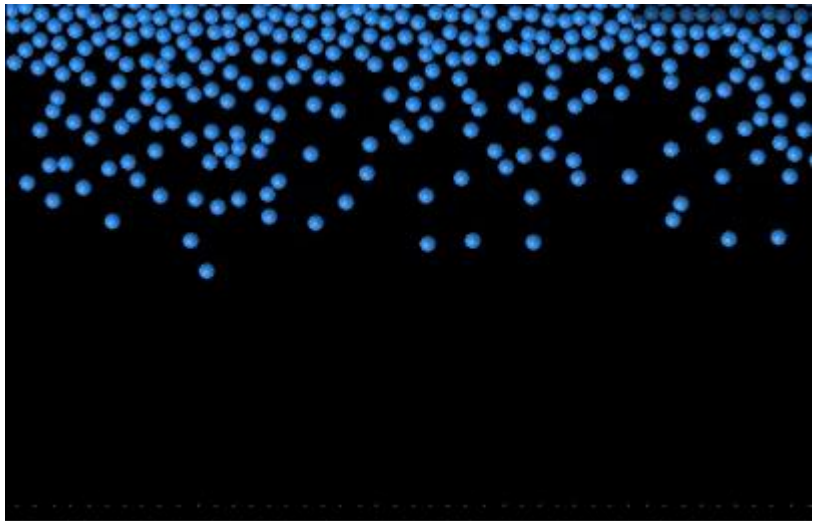

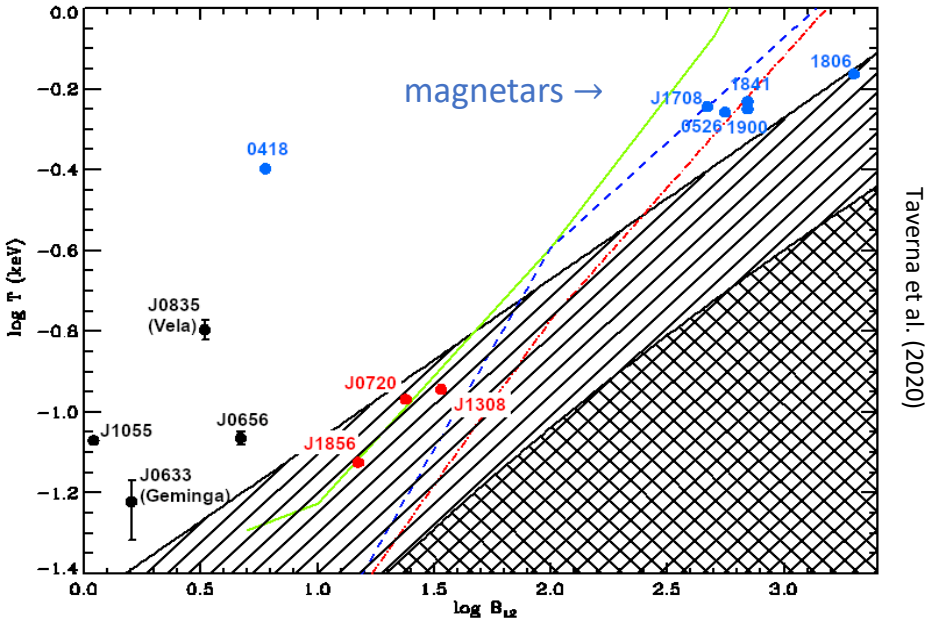

Taverna et al. (2020)

Surface emission models

- Surface photons reprocessed by a standard, magnetized atmosphere → high PD (X-mode)
- Very strong B-fields elongate atoms along the field direction → molecular chains are formed for sufficiently low T
- The atmosphere settles onto the surface and the (condensed) crust is left exposed
- Much lower PD (both O- and X-)

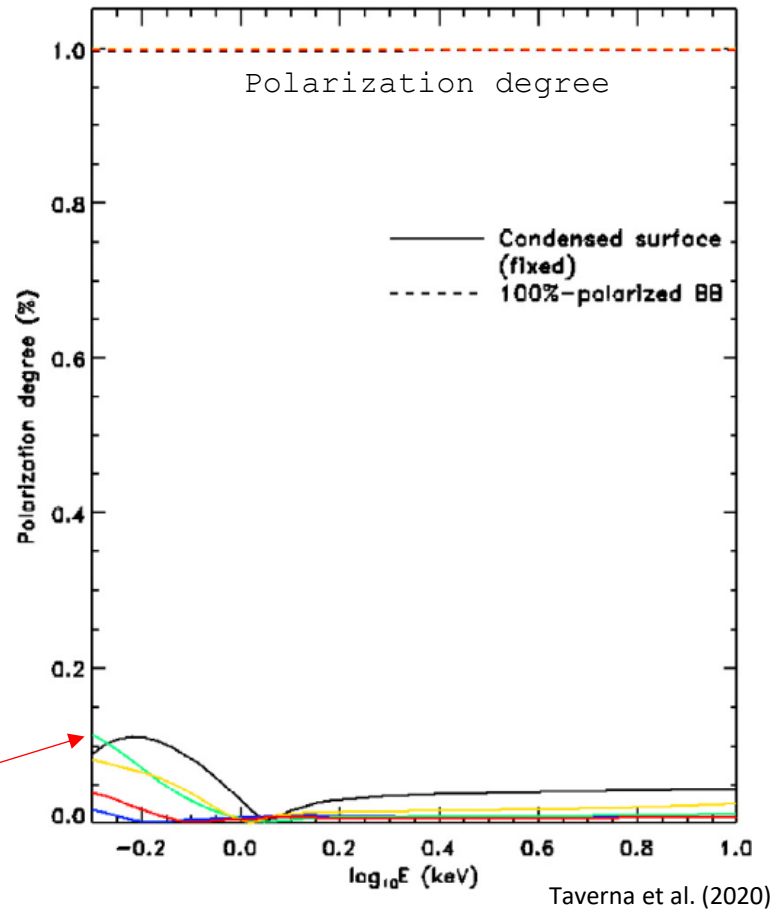

$\mathrm{PD} \lesssim 20\%$

Taverna et al. (2020)

AXP 4U 0142+61

- Brightest among persistent magnetars
- $B_{P\dot{P}} \approx 1.5 \times 10^{14}$ G
- Spectrum BB+PL
  - $kT_{\rm BB} = 0.471^{+0.004}_{-0.004}$ keV
  - $\Gamma = 3.69^{+0.05}_{-0.05}$
  - $\chi^2/{\rm dof} = 511.5/441$

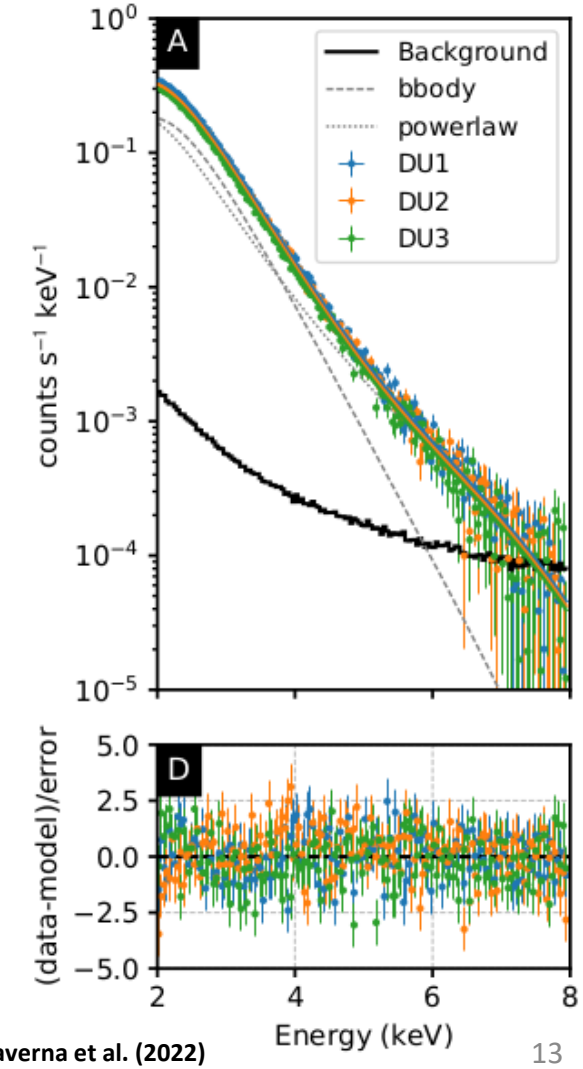

Taverna et al. (2022)

AXP 4U 0142+61

- Brightest among persistent magnetars
- $B_{P\dot{P}} \approx 1.5 \times 10^{14}$ G
- Spectrum BB+PL
- Polarization measurement (840 ks):
  - PD $= 13.5\%$ (17σ) – PA $\approx 50°$ E ($\mathrm{MDP}_{99} \approx 2\%$)
  - Complex behavior against photon energy

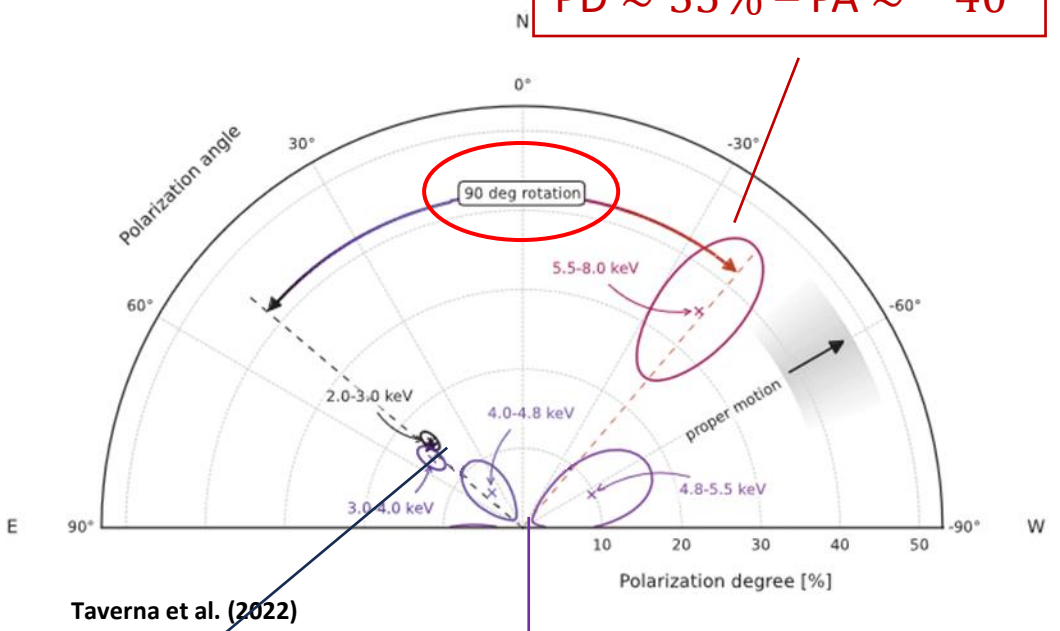

Taverna et al. (2022)

High energies
PD $\approx 35\%$ – PA $\approx -40°$

Low energies
PD $\approx 15\%$ – PA $\approx 50°$

4–5 keV
PD ≈ 0

4U 0142+61 – Summary

- 90°-swing → X- and O- modes ⇒ **$\boldsymbol{B}$-field should be ultra-strong ($\gtrsim 10^{13}$ G)**
- PD at high energies $\approx 35\%$ ⇒ **PL tail populated by RCS photons ($\approx 33\%$)**
  Magnetar model reliable!
- Low PD at low energies ⇒ **Condensed surface exposed**

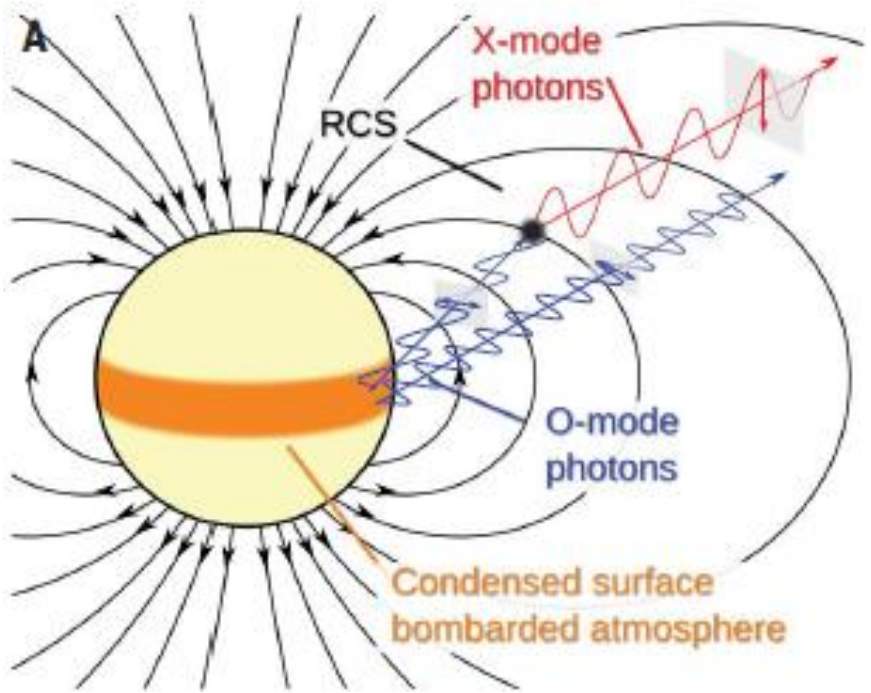

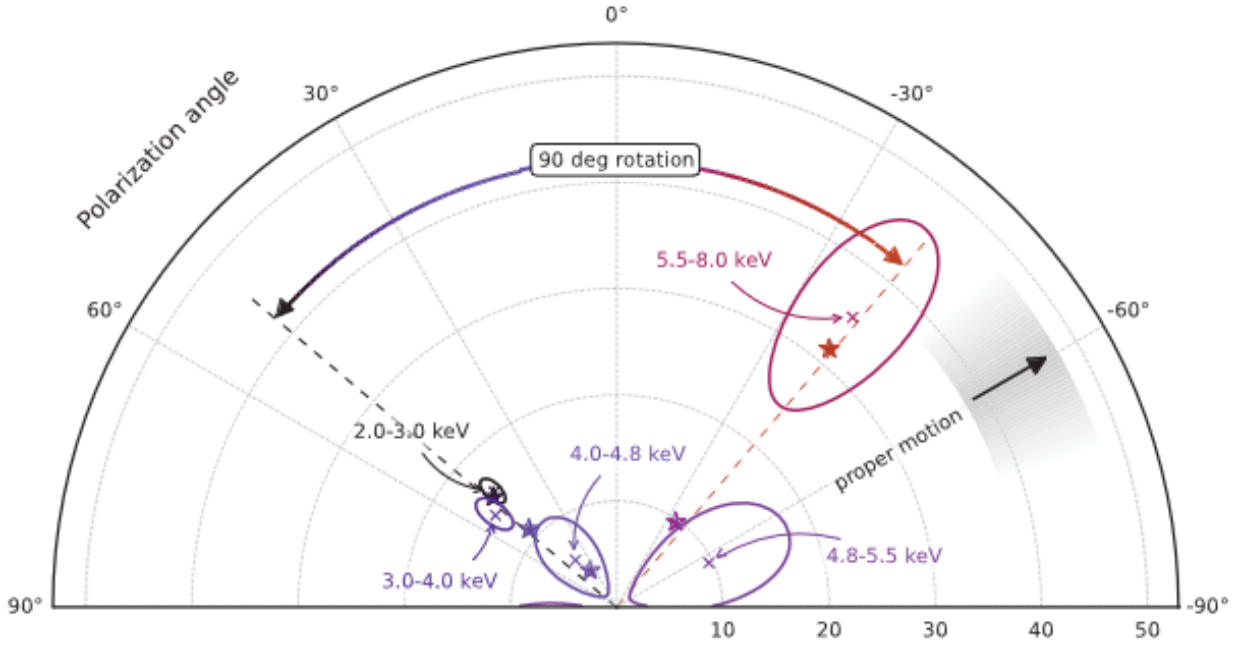

Taverna et al. (2022)

★ Numerical simulation

- Mode switching in 4U 0142+61 as a consequence of partial mode conversion at the vacuum resonance (Lai 2023)

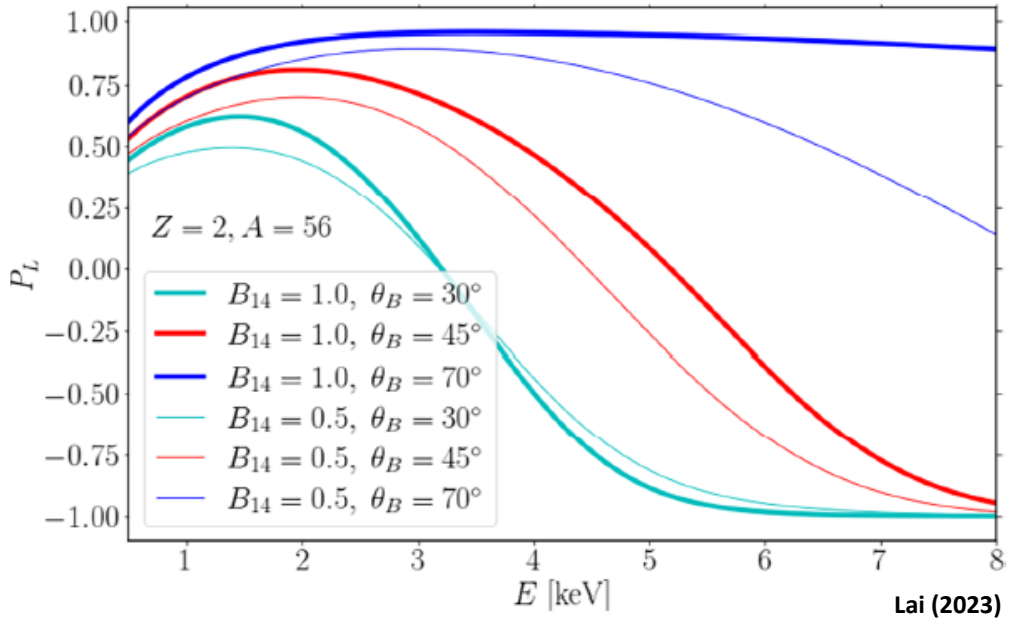

Lai (2023)

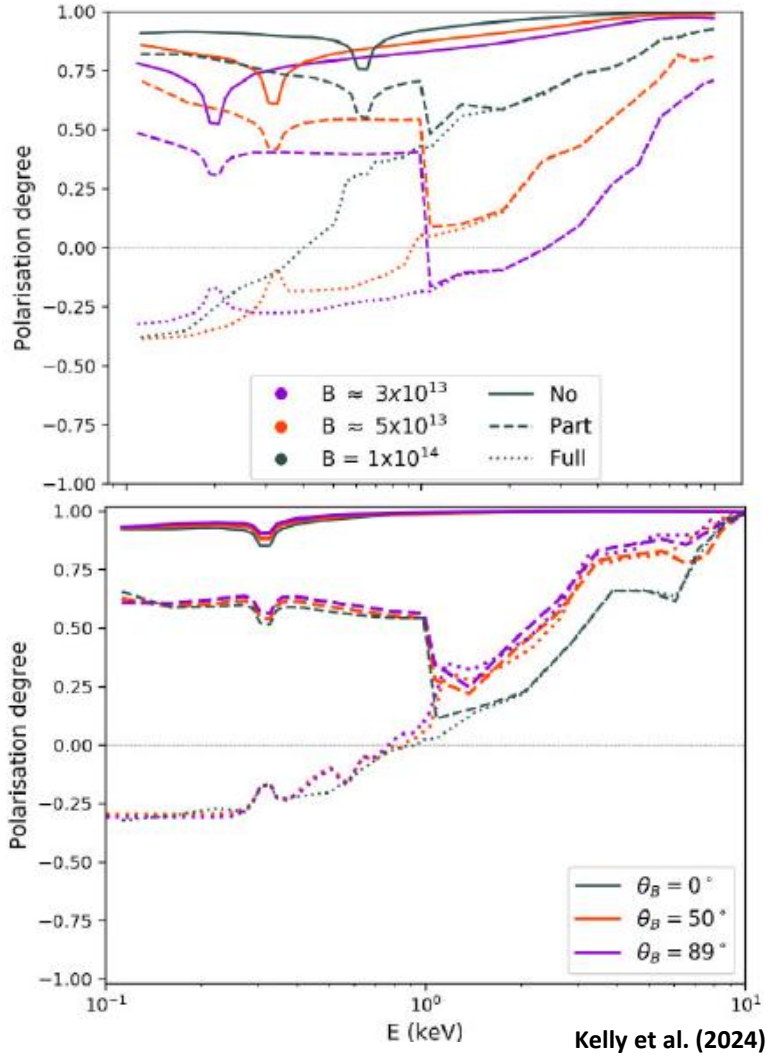

Kelly et al. (2024)

- Not without problems (once scattering/free-free and integration over the whole surface are considered ⇒ no mode switching in the IXPE band)

4U 0142+61 – Summary

- 90°-swing → X- and O- modes ⇒ **B-field should be ultra-strong ($\gtrsim 10^{13}$ G)**
- PD at high energies $\approx 35\%$ ⇒ **PL tail populated by RCS photons ($\approx 33\%$)**
  Magnetar model reliable!
- Low PD at low energies ⇒ **Condensed surface exposed**

What about vacuum birefringence?

AXP 4U 0142+61 – Phase resolved

- Low phase-averaged PD (< 40%) ⇒ Vacuum birefringence cannot be probed

- Phase dependent results
  - PD is in-phase with the LC (determined at the surface)
  - PA is sinusoidal (RVM)

- RVM for extended regions holds for dipolar fields only
  - In the magnetar model B is dipolar only far away from the surface

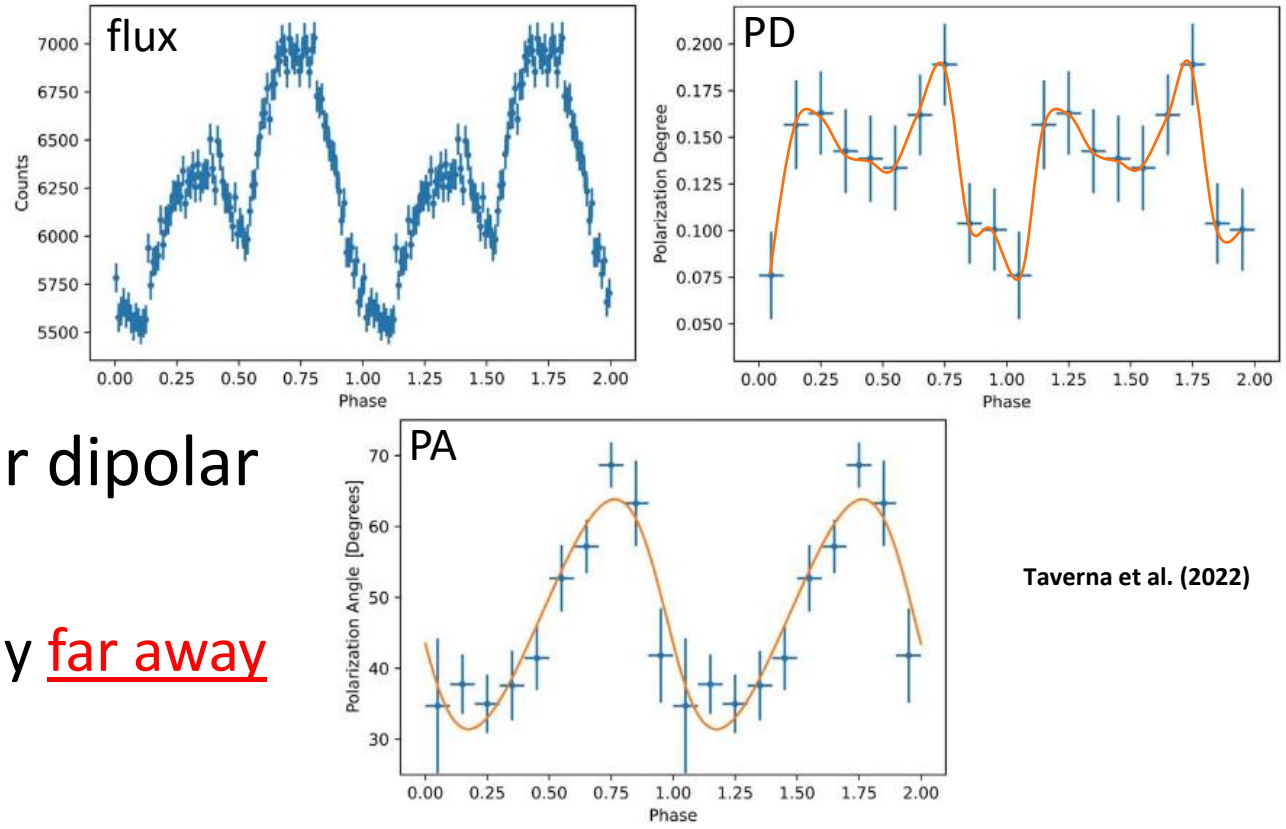

Taverna et al. (2022)

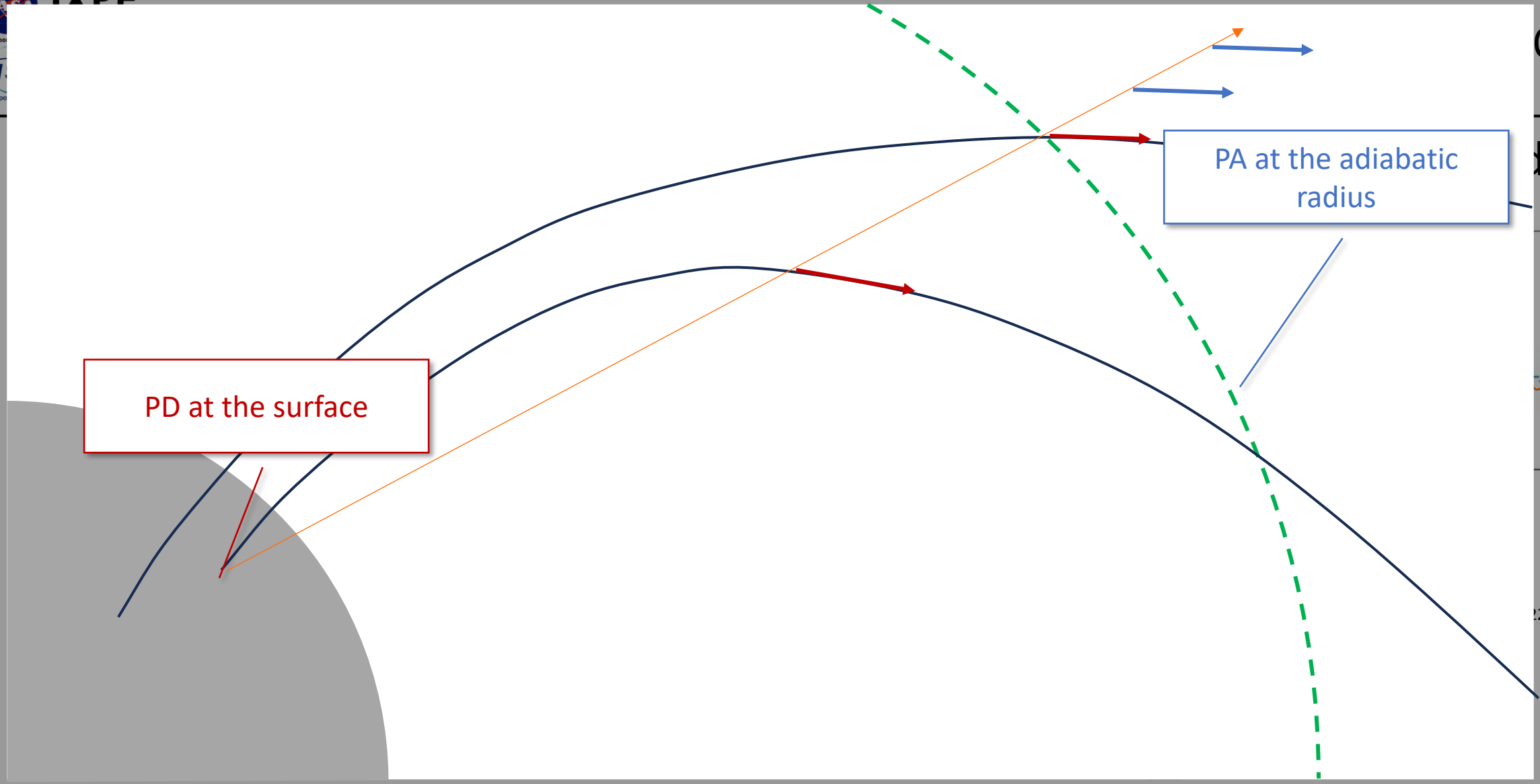
PA at the adiabatic radius
PD at the surface

AXP 1RXS J170849.0–4009100

- 2nd brightest magnetar
- $B_{P\dot{P}} \approx 5 \times 10^{14}$ G
- Spectrum BB+PL or BB+BB?
  - BB+PL – $kT_{\mathrm{BB}} = 0.454^{+0.007}_{-0.006}$ keV
    $\Gamma = 2.97^{+0.009}_{-0.056}$
    $\chi^2 = 410.8/408$ dof
  - BB+BB – $kT_{\mathrm{BB}_1} = 0.435^{+0.007}_{-0.007}$ keV
    $kT_{\mathrm{BB}_2} = 1.073^{+0.031}_{-0.029}$
    $\chi^2 = 405.8/408$ dof

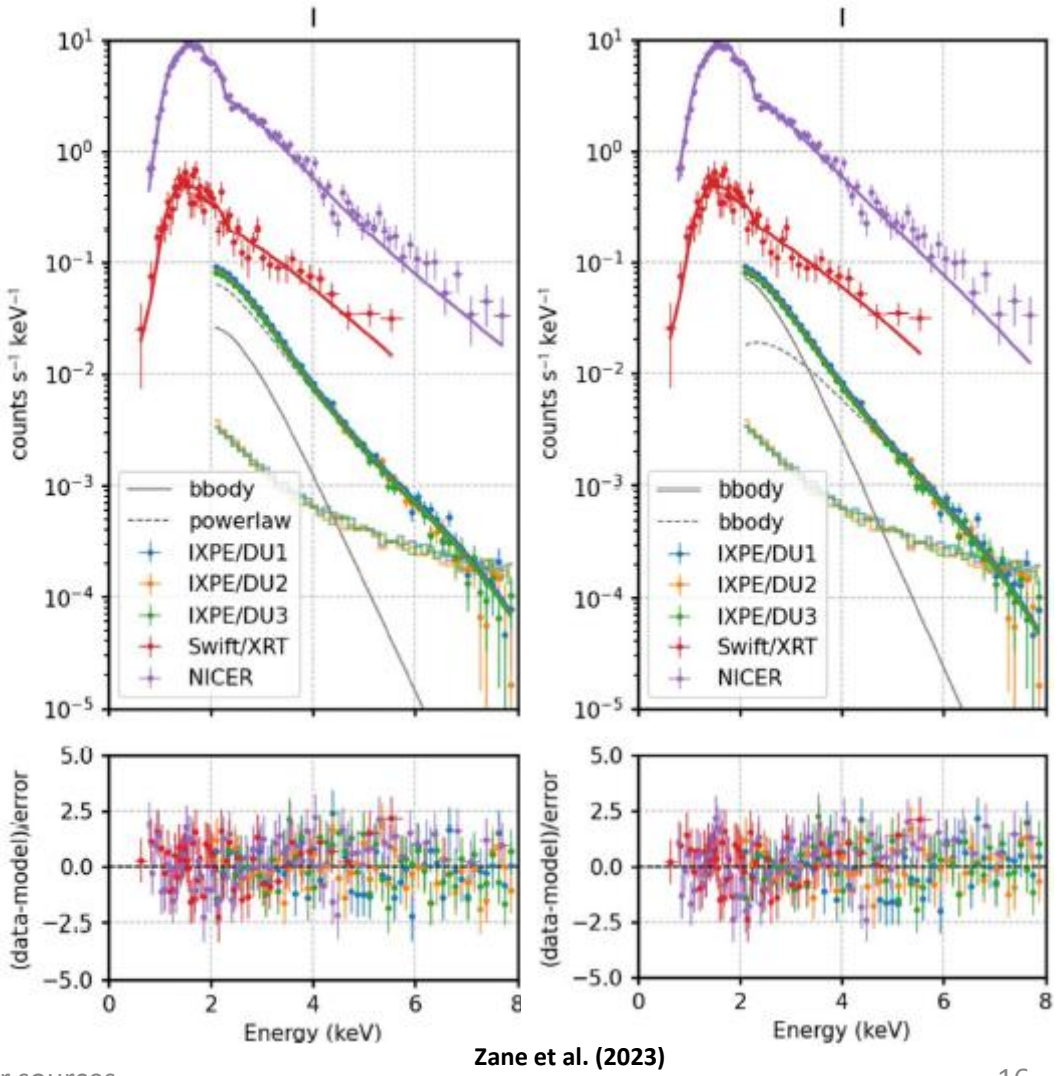

Zane et al. (2023)

AXP 1RXS J170849.0–4009100

- 2nd brightest magnetar
- $B_{P\dot{P}} \approx 5 \times 10^{14}$ G
- Spectrum BB+PL or BB+BB?
- Polarization measurement (837 ks):
  - PD = 35% (22.5σ) – PA $\approx 60°$ W
  - Polarization direction is constant in the IXPE band
  - PD at 6–8 keV: $\approx 85\%$ ($\mathrm{MDP}_{99} = 50\%$)

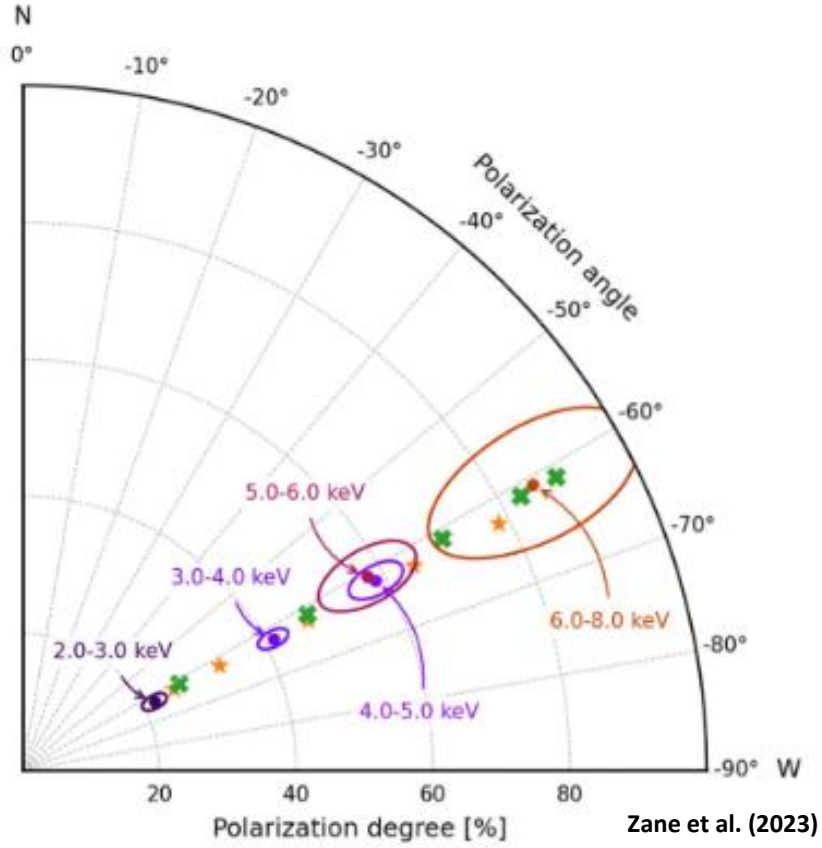

Zane et al. (2023)

AXP 1RXS J170849.0–4009100

- 2nd brightest magnetar
- $B_{P\dot{P}} \approx 5 \times 10^{14}$ G
- Spectrum BB+PL or BB+BB?
- Polarization measurement (837 ks):
  - PD = 35% (22.5σ) – PA $\approx 60°$ W
  - Polarization direction is constant in the IXPE band
  - PD at 6–8 keV: $\approx 85\%$ ($\mathrm{MDP}_{99} = 50\%$)

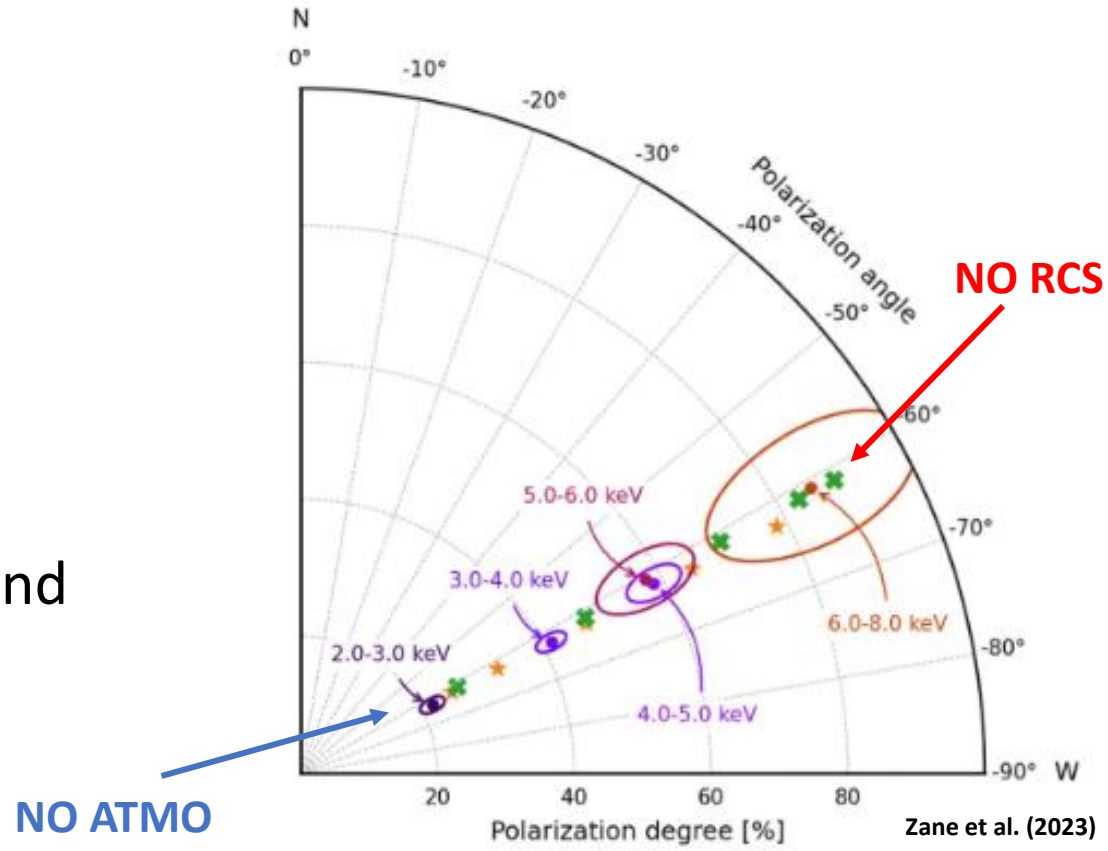

Zane et al. (2023)

Interpretation (Zane et al. 2023)

- Phase transition across the surface

CAP+BELT model

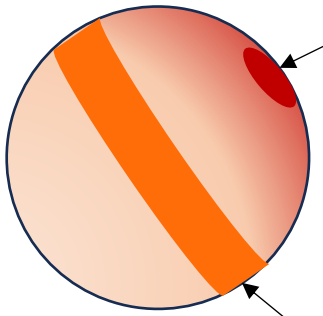

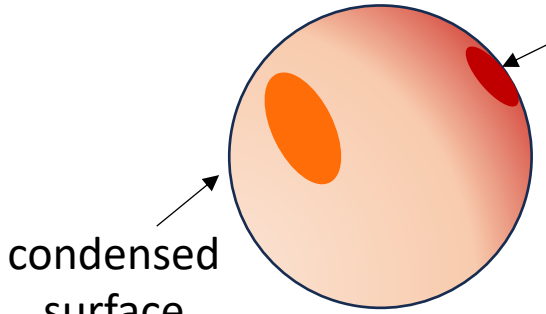

2 CAPS model

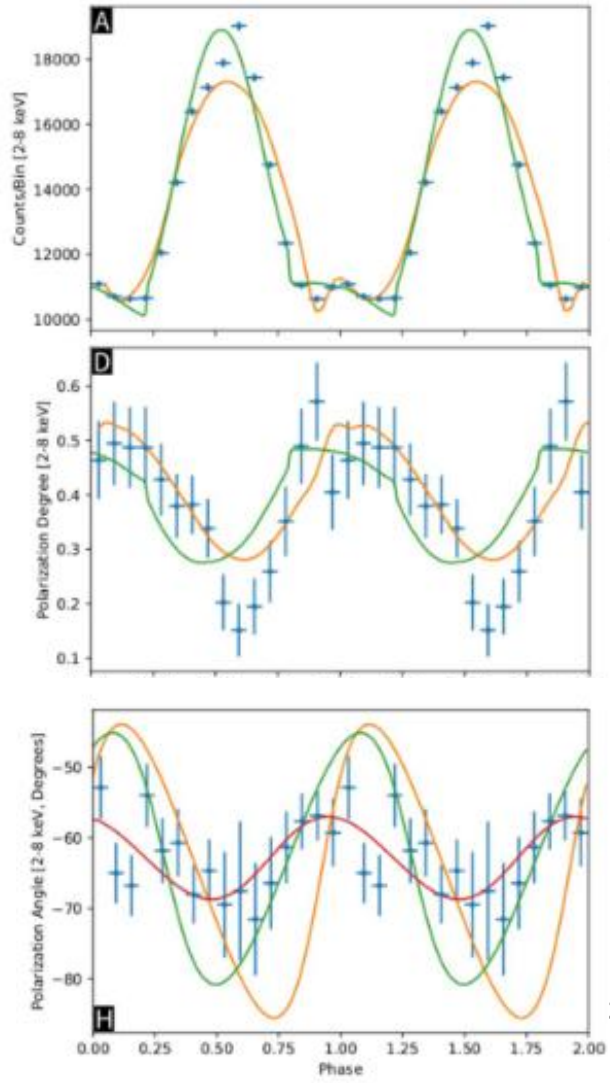

CAP+BELT

2 CAPS

Zane et al. (2023)

SGR 1806–20

- Emitted the strongest giant flare ever detected (December 27, 2004)
- $B_{P\dot{P}} \approx 8 \times 10^{14}$ G (strongest B-field)
- Observed 1 month after an active phase (emission of a bunch of bursts)
- Flux lowered wrt quiescence ($\approx 10^{-12}$ erg cm^{-2} s^{-1}, 1/10 than tabulated)
- Contamination by solar flares during IXPE observation

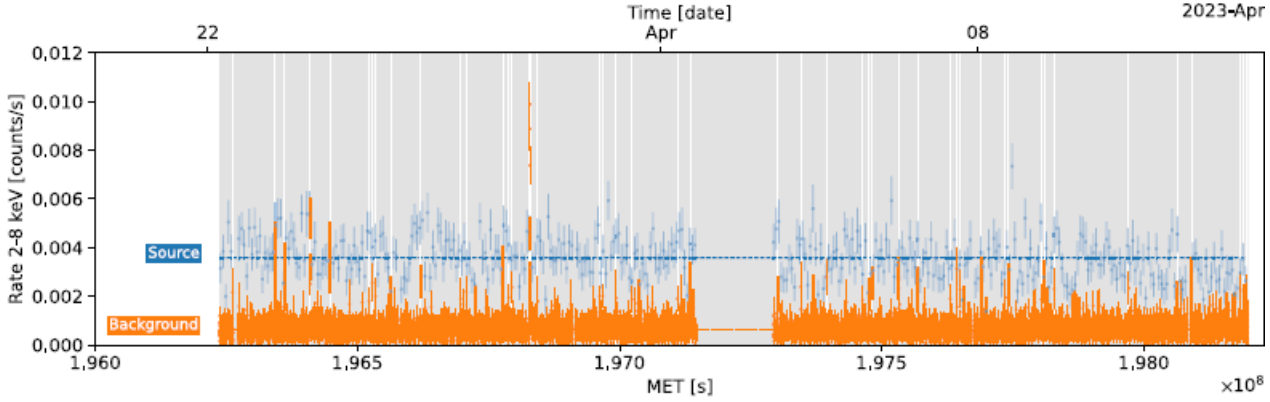

Turolla et al. (2023)

Observation (Turolla et al. 2023)

- XMM DDT observation
  - BB+PL spectral decomposition ($kT_{\rm BB} = 0.59 \pm 0.04$ keV, $\Gamma = 1.7 \pm 0.1$)
  - Double-peaked pulse profile ($\rm P.F. \approx 5\%$)

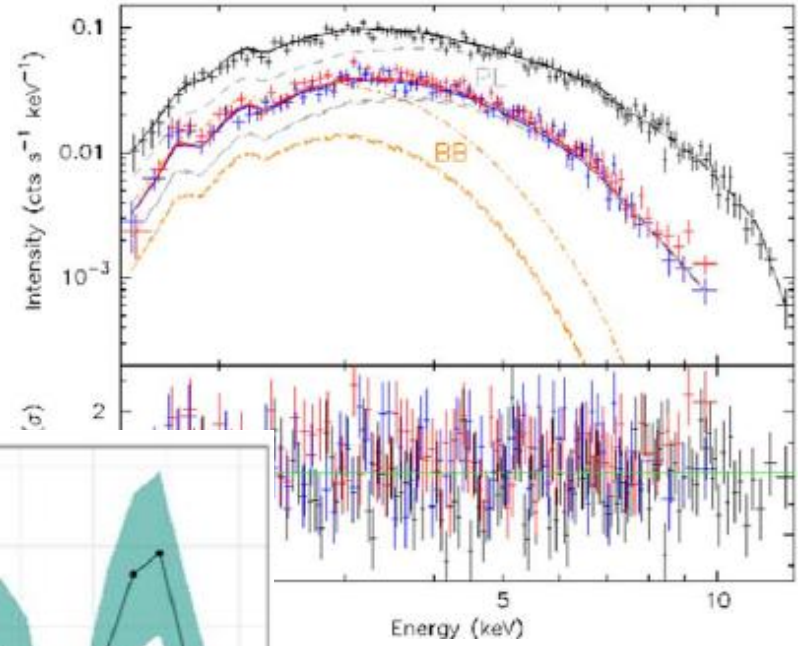

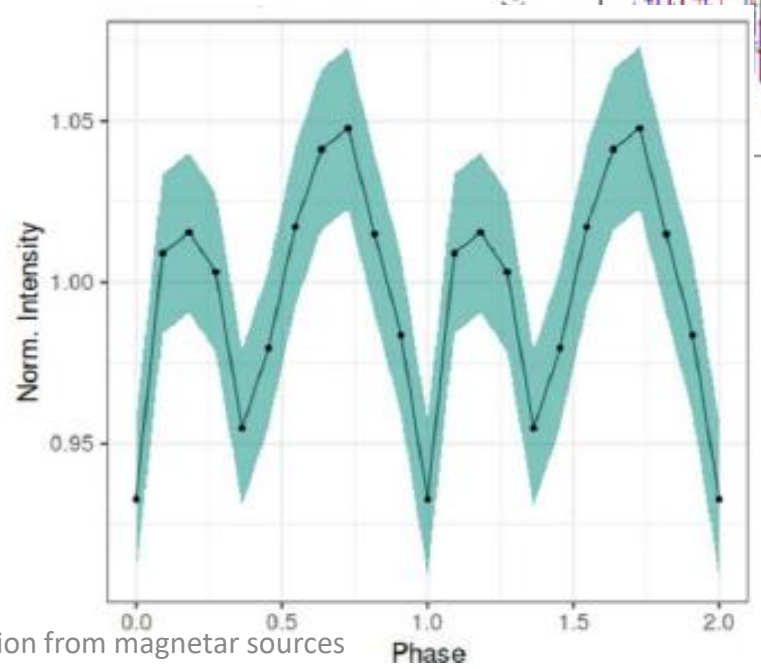

Turolla et al. (2023)

Observation (Turolla et al. 2023)

- XMM DDT observation
  - BB+PL spectral decomposition ($kT_{\rm BB} = 0.59 \pm 0.04$ keV, $\Gamma = 1.7 \pm 0.1$)
  - Double-peaked pulse profile (P. F. $\approx 5\%$)
- IXPE observation (947 ks)
  - 2-8 keV – PD $\sim 6\%$ (MDP$_{99} \approx 20\%$)
  - Energy-dependent PD

    $\lesssim 24\%$ (2–4 keV, 3σ u.l.)

    $= 31.6 \pm 10.5\%$ (4–5 keV, 99% c.l. detection only «probable»)

    $\lesssim 55\%$ (5–8 keV, 3σ u.l.)

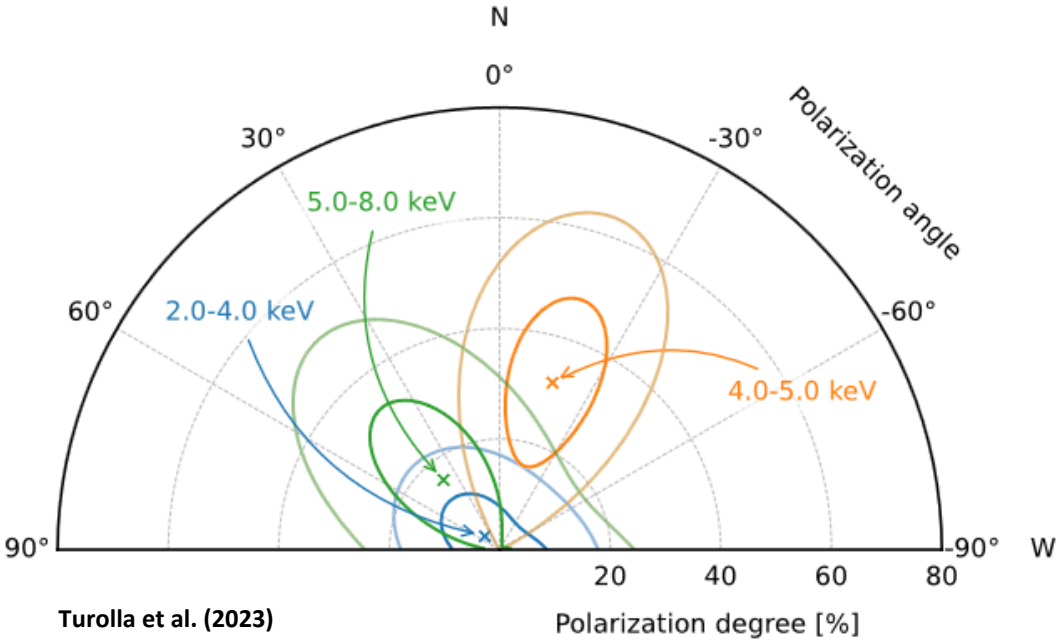

Turolla et al. (2023)

AXP 1E 2259+586

- $B_{P\dot{P}} \approx 6 \times 10^{13}$ G (low-B)
- Spectral fit BB+PL is not good enough → adding an **absorption line** (Pizzocaro+19) improves the fit
- XMM contemporary observation

	$kT_{\rm BB}$ (keV)	Γ	$E_{\rm line}$ (keV)	$\sigma_{\rm line}$ (keV)	χ^2/dof
XMM	0.44 ± 0.01	4.09 ± 0.08	$0.96^{+0.07}_{-0.18}$	$0.23^{+0.10}_{-0.06}$	94.1/93
IXPE	0.43 ± 0.01	4.36 ± 0.09	frozen	frozen	138.0/147

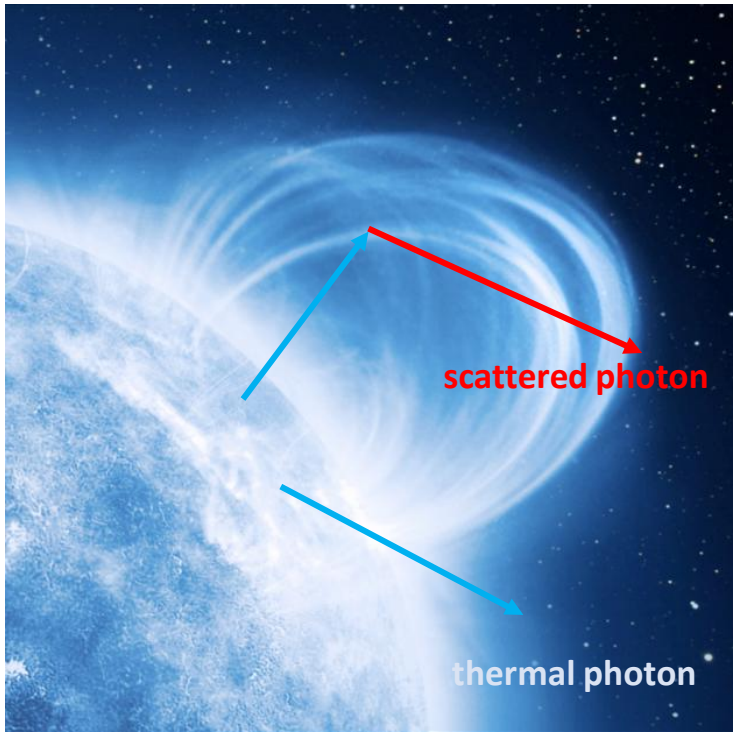

Credit: ESA Science & Technology

Observation (Heyl et al. 2024)

- IXPE phase-dependent observation (1.2 Ms)
  - Polarization up to $\approx 30\%$ (well above MDP_{99}) at particular phases (corresponding to the rise and maximum of the primary LC peak)
  - Secondary peak basically unpolarized
  - PA well fitted by a RVM in which photons are assumed to change mode (from O- to X- and vice versa)

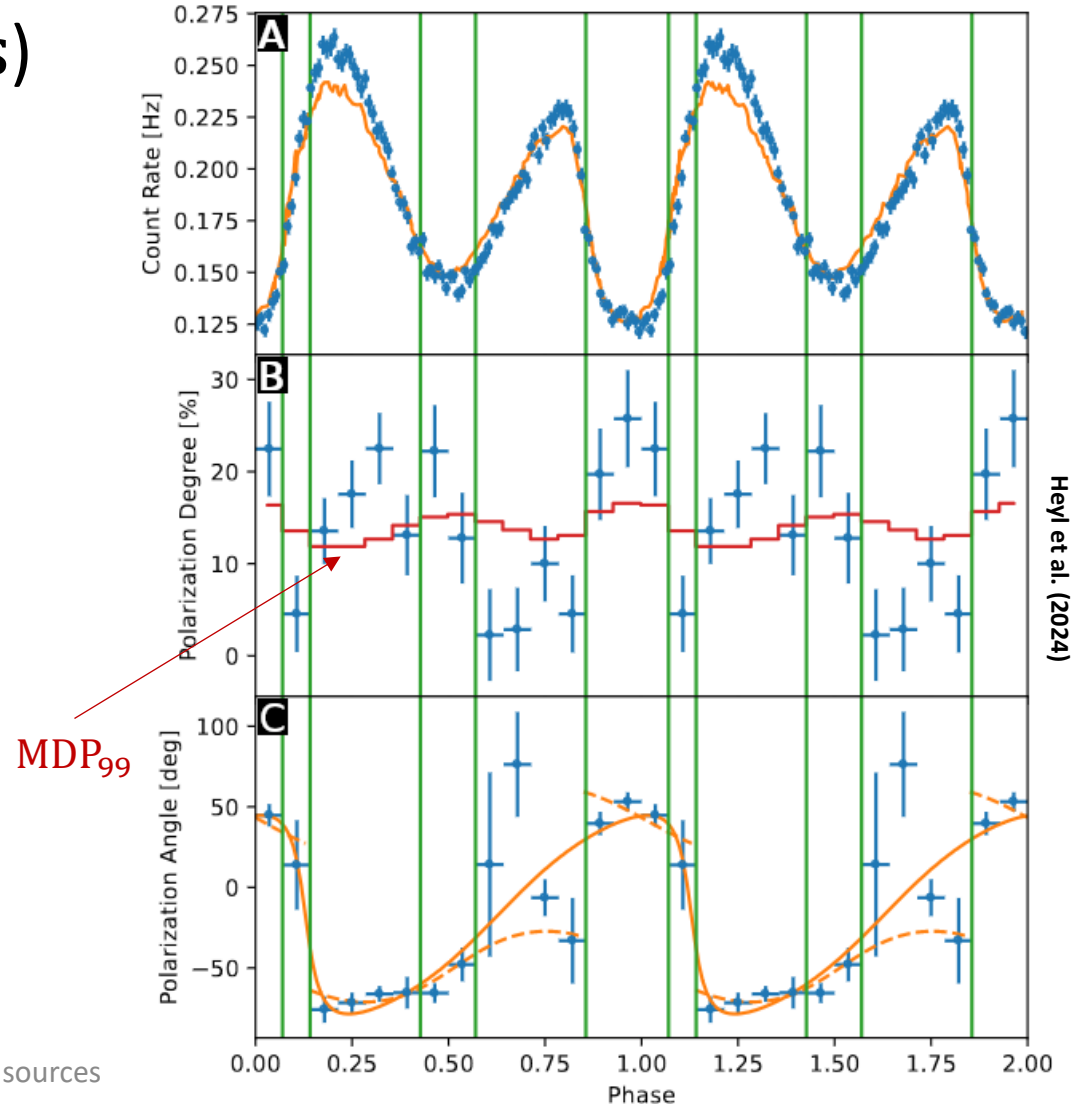

Interpretation (Heyl et al. 2024)

- Theoretical interpretation (in terms of the magnetic-loop model)

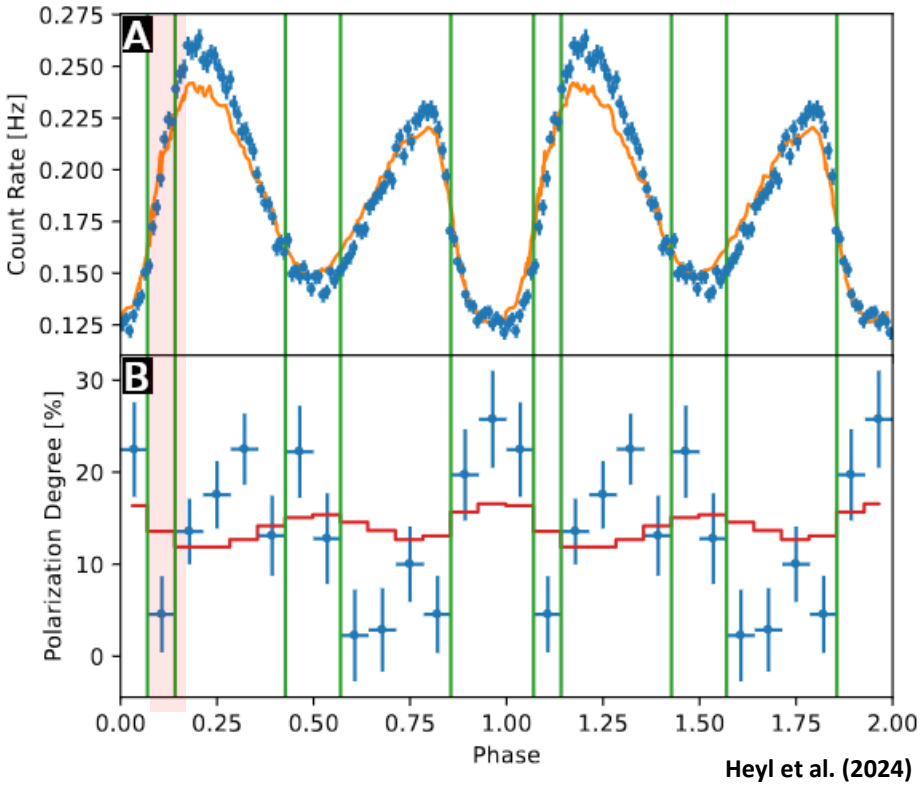

Heyl et al. (2024)

1st rise

- unscattered (O-mode) photons (lowly polarized) are directly intercepted
- scattered photons (at most 33% X-mode) are deviated away from the LOS

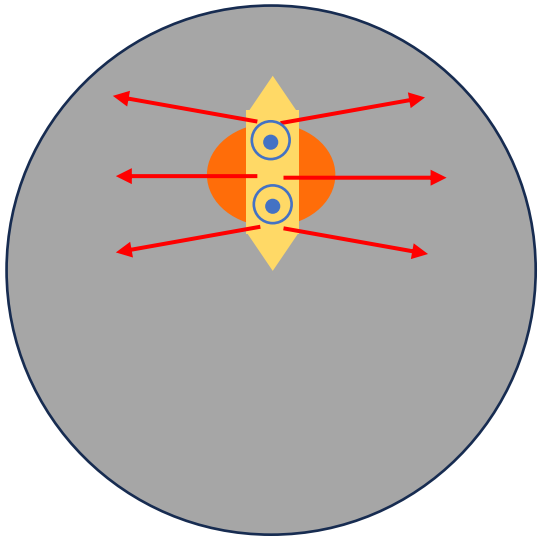

Interpretation (Heyl et al. 2024)

- Theoretical interpretation (in terms of the magnetic-loop model)

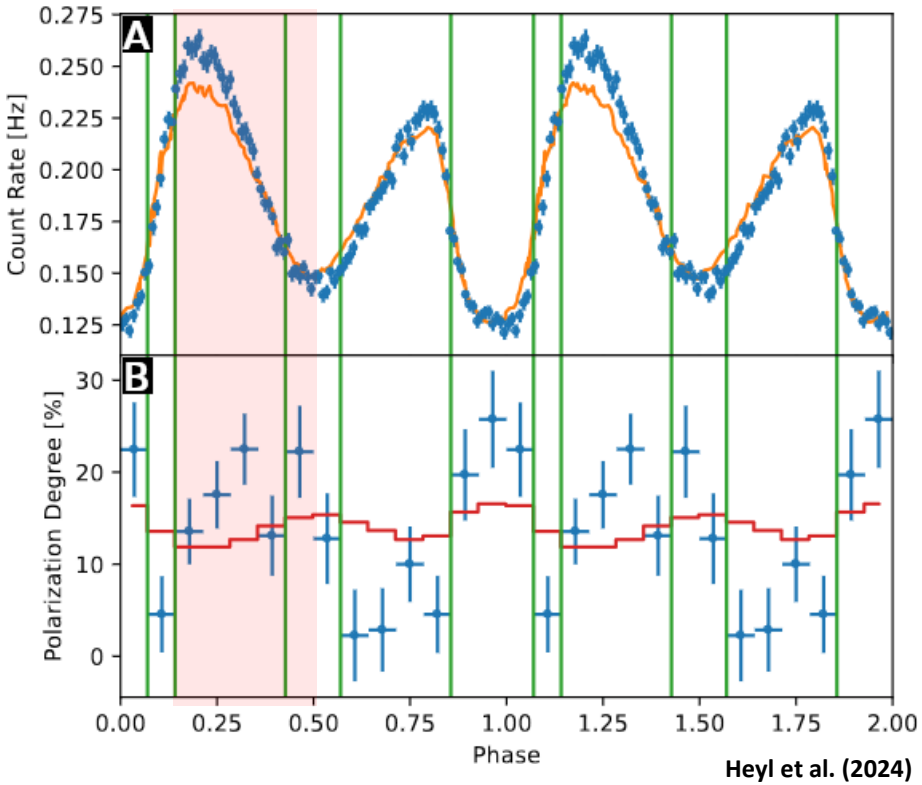

Heyl et al. (2024)

1st peak

- scattered X-mode photons are now intercepted (with also primary O-mode ones from the underlying spot → peak in the flux)
- polarization increases
- contamination from O-mode condensed-surface photons prevent PD to reach 33%

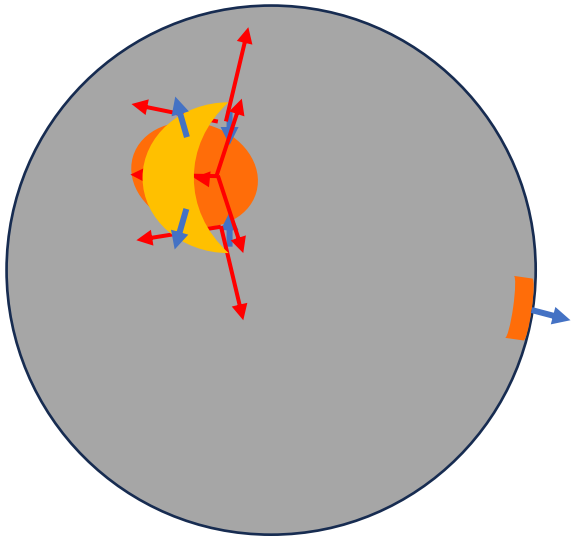

Interpretation (Heyl et al. 2024)

- Theoretical interpretation (in terms of the magnetic-loop model)

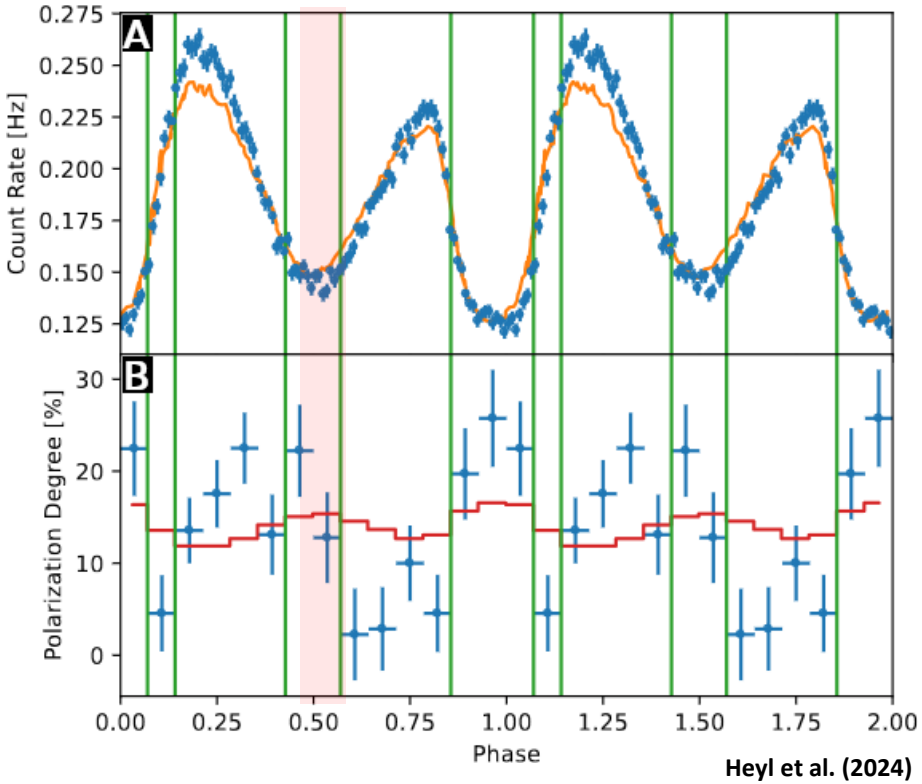

Heyl et al. (2024)

Little dip

- the larger spot starts to be hidden behind (only a fraction of mildly polarized photons are observed)
- the secondary spot (with no loop) enters in view (emitting low-polarized O-mode photons)

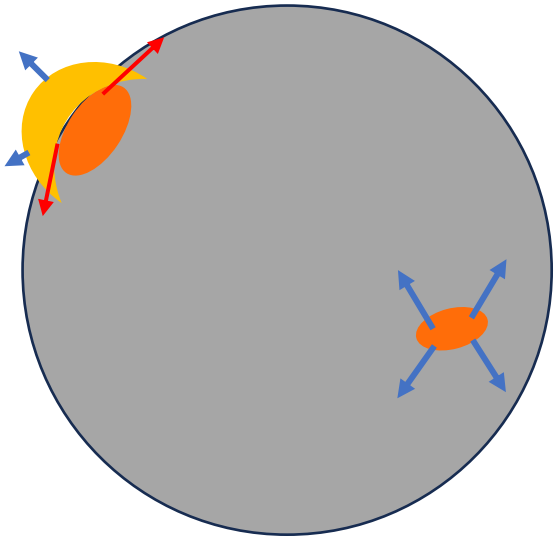

Interpretation (Heyl et al. 2024)

- Theoretical interpretation (in terms of the magnetic-loop model)

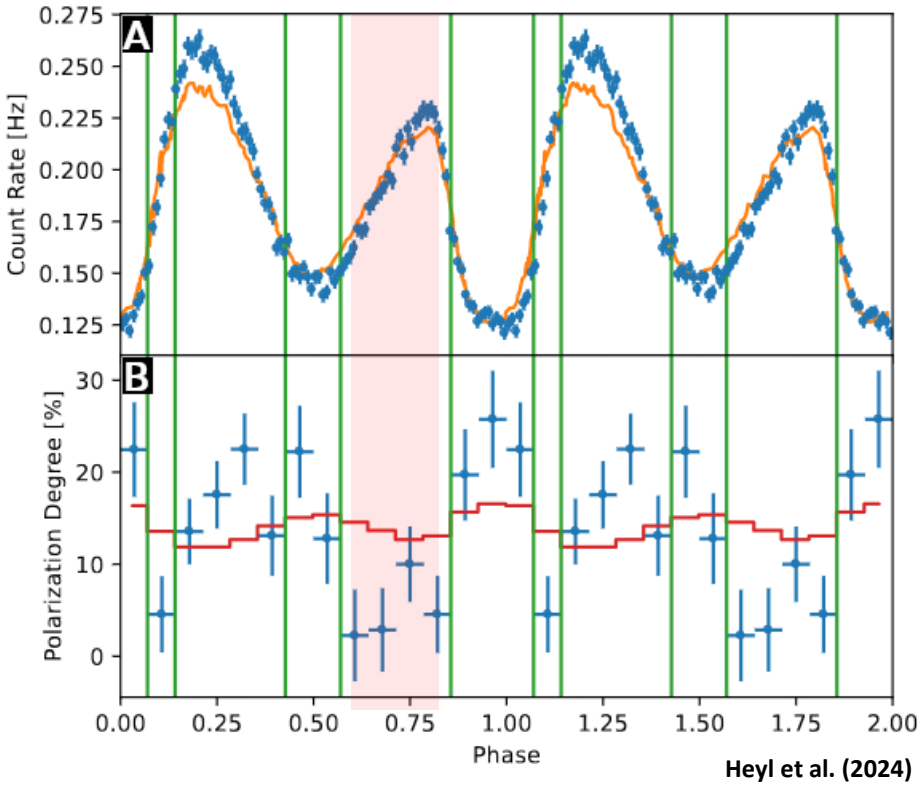

Heyl et al. (2024)

2nd peak

- the secondary spot is fully in view (peak in the flux)
- only condensed-surface photons collected (O-mode, polarized at no more than 10–15%)

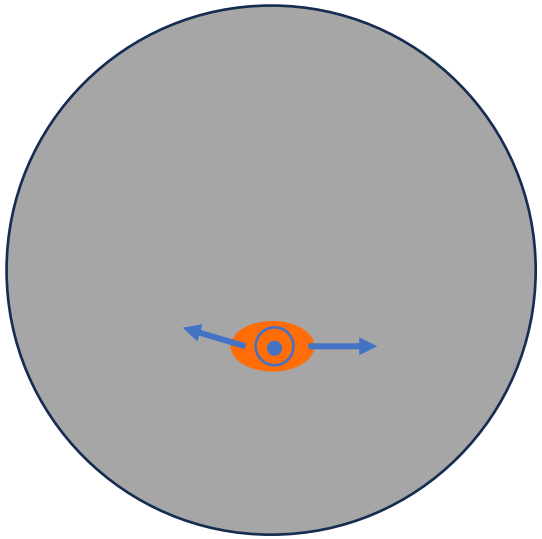

Interpretation (Heyl et al. 2024)

- Theoretical interpretation (in terms of the magnetic-loop model)

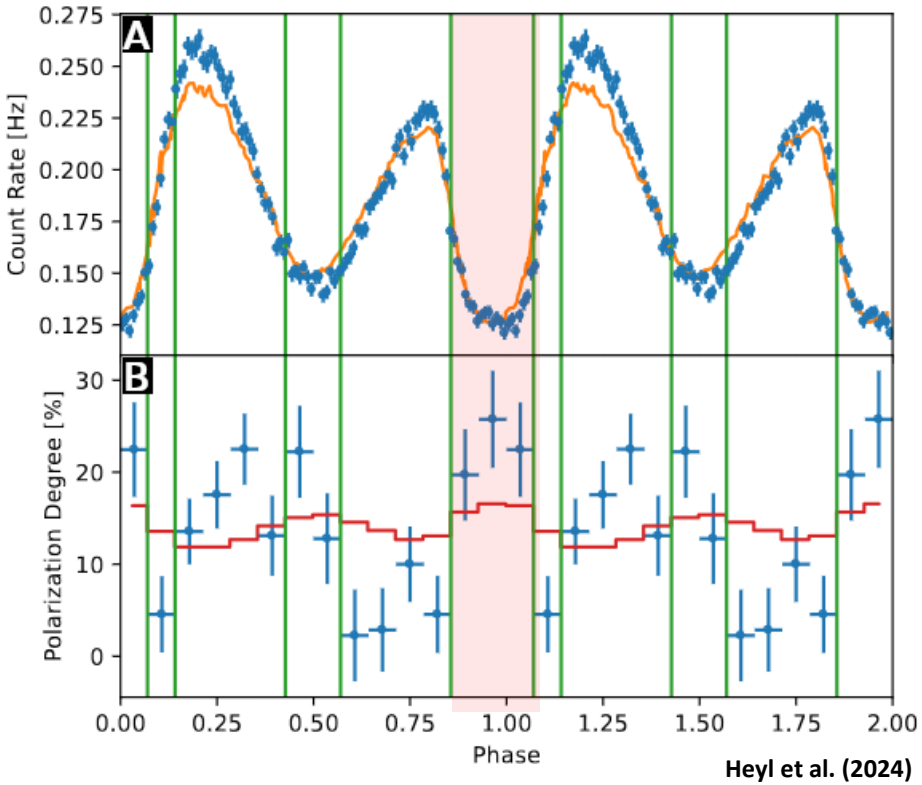

Big dip

- secondary spot photons are not in view
- the primary peak returns in view
- X-mode scattered photons along the LOS are intercepted first (minimum in the flux, maximum in PD)

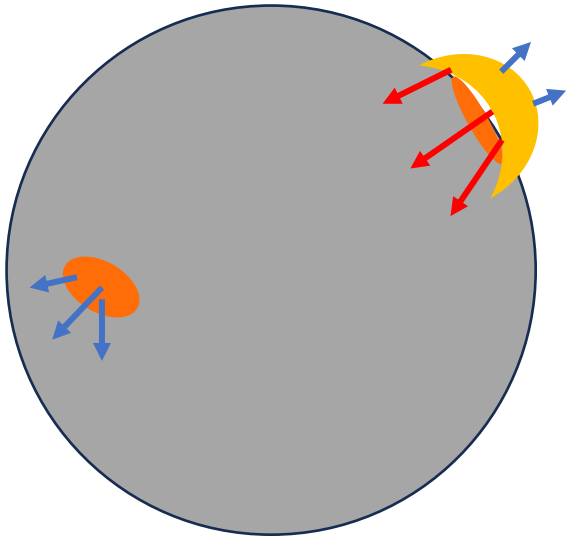

Conclusions

- X-ray polarimetry on magnetar sources complemented information from spectral and timing analysis
- Detection of photons polarized in two normal modes in 4U 0142 confirmed the presence of strong magnetic fields ($\gtrsim 5 \times 10^{13}$ G) independently of $P\dot{P}$
- Energy-dependent PD and PA allowed to confirm the expectations of the RCS model
- Phase-dependent PD and PA provided a first hint that vacuum birefringence effects are at work around magnetars
- Further magnetars should be explored in polarized X-rays (persistent and transient in outburst, softer X-ray energies)

Thanks!

Backup slides

Vacuum birefringence – Extension of emitting regions

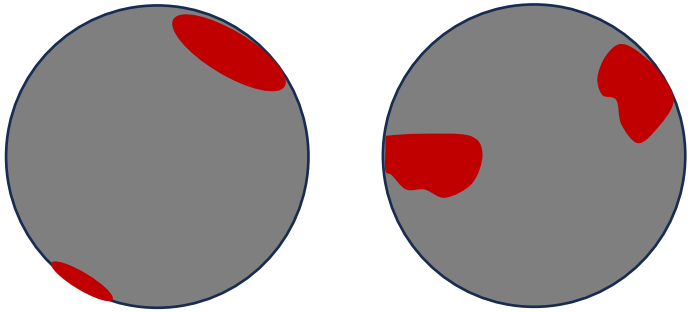

If emitting regions on the surface are small depolarization due to the tangled magnetic field is not much effective (van Adelsberg & Perna 09)

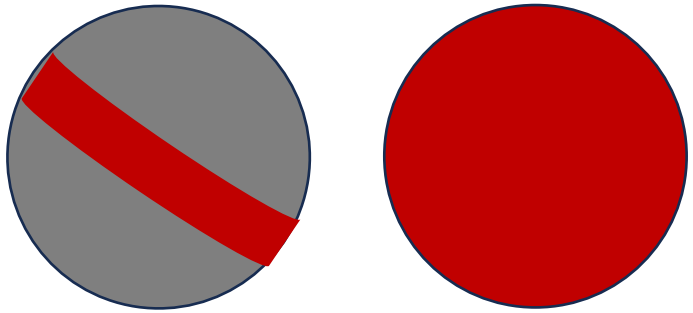

For large emitting regions (or the entire surface) geometrical depolarization may be much more important (surface 100% → 40% at infinity, Taverna+ 20)

CS vs ATMO – Removing spectral degeneracy

- Spectra for atmosphere and condensed-surface model are similar (BB-like)

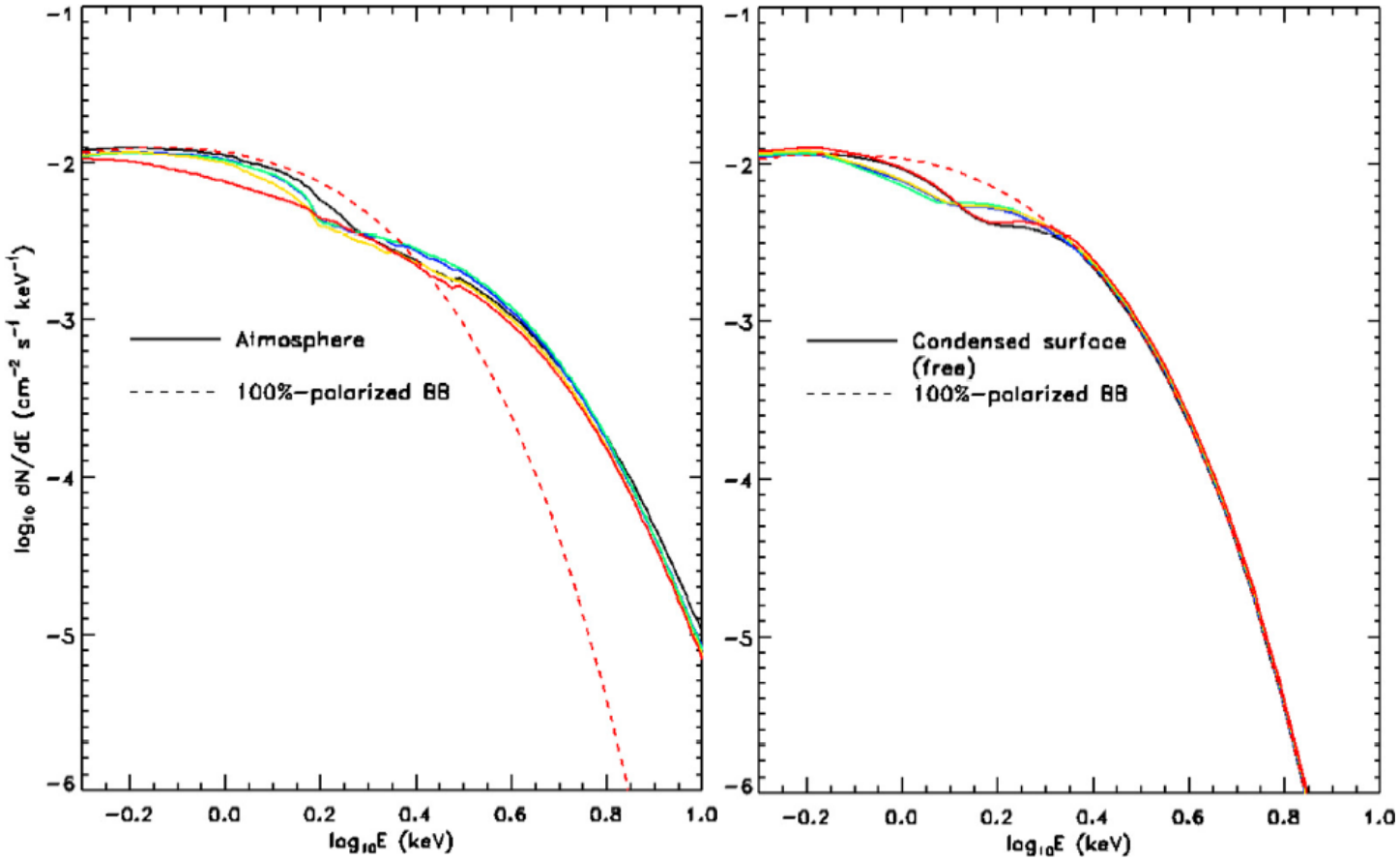

Taverna et al. (2020)

CS vs ATMO – Removing spectral degeneracy

- Spectra for atmosphere and condensed-surface model are similar (BB-like)
- Different behaviors of PA with energy are expected for particular emission models and geometries

«standard» atmosphere

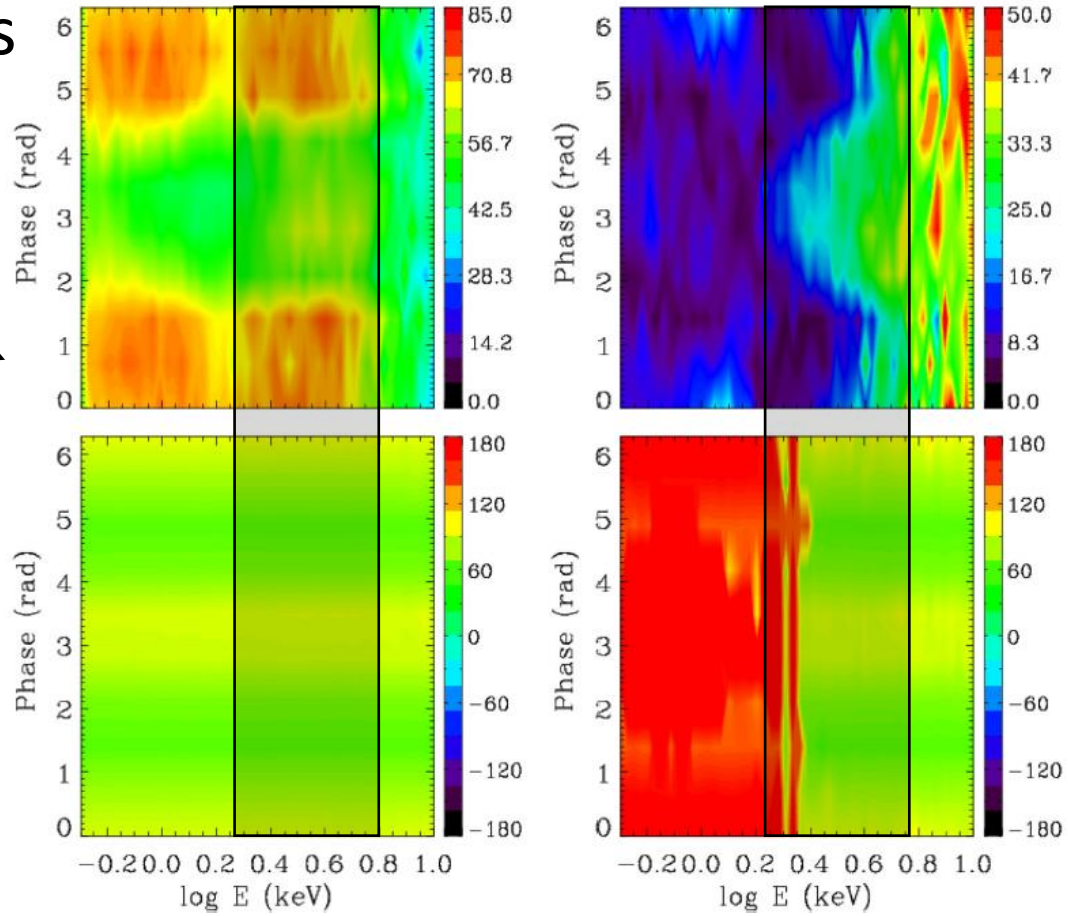

IXPE band

condensed surface

Taverna et al. (2020)

IXPE magnetar targets

- **AXP 4U 0142+61** (R.A. 01:46:22.41, DEC. 61°45’03’’.2)
  - Cassiopeia – Distance: 3.6 kpc
  - January 31st – February 27th 2022 (840 ks)
  - Unabsorbed flux (2–10 keV): 6×10^{-11} erg cm^{-2} s^{-1}
- **AXP 1RXS J170849.0–4009100** (R.A. 17:08:46.3, DEC. –40°08’44’’.6)
  - Scorpio – Distance: 5–10 kpc
  - September 19th – October 8th 2022 (837 ks)
  - Unabsorbed flux (2–10 keV): 2.4×10^{-11} erg cm^{-2} s^{-1}
- **SGR 1806–20** (R.A. 18:08:39.8, DEC. –20°24’26’’.7)
  - Sagittarius – Distance: 8.7 kpc
  - March 22nd – April 13th 2023 (947 ks)
  - Unabsorbed flux (2–10 keV): 4×10^{-12} erg cm^{-2} s^{-1}

IXPE magnetar targets

- **AXP 1E 2259+586** (R.A. 23:01:08.8, DEC. 58°52’20’’.8)
  - Cassiopeia – Distance: 3.2 kpc
  - June 2nd – July 6th 2023 (1.2 Ms)
  - Unabsorbed flux (2–10 keV): 1.4×10^{-11} erg cm^{-2} s^{-1}

1RXS J170849.0–4009100

- Phase-dependent results

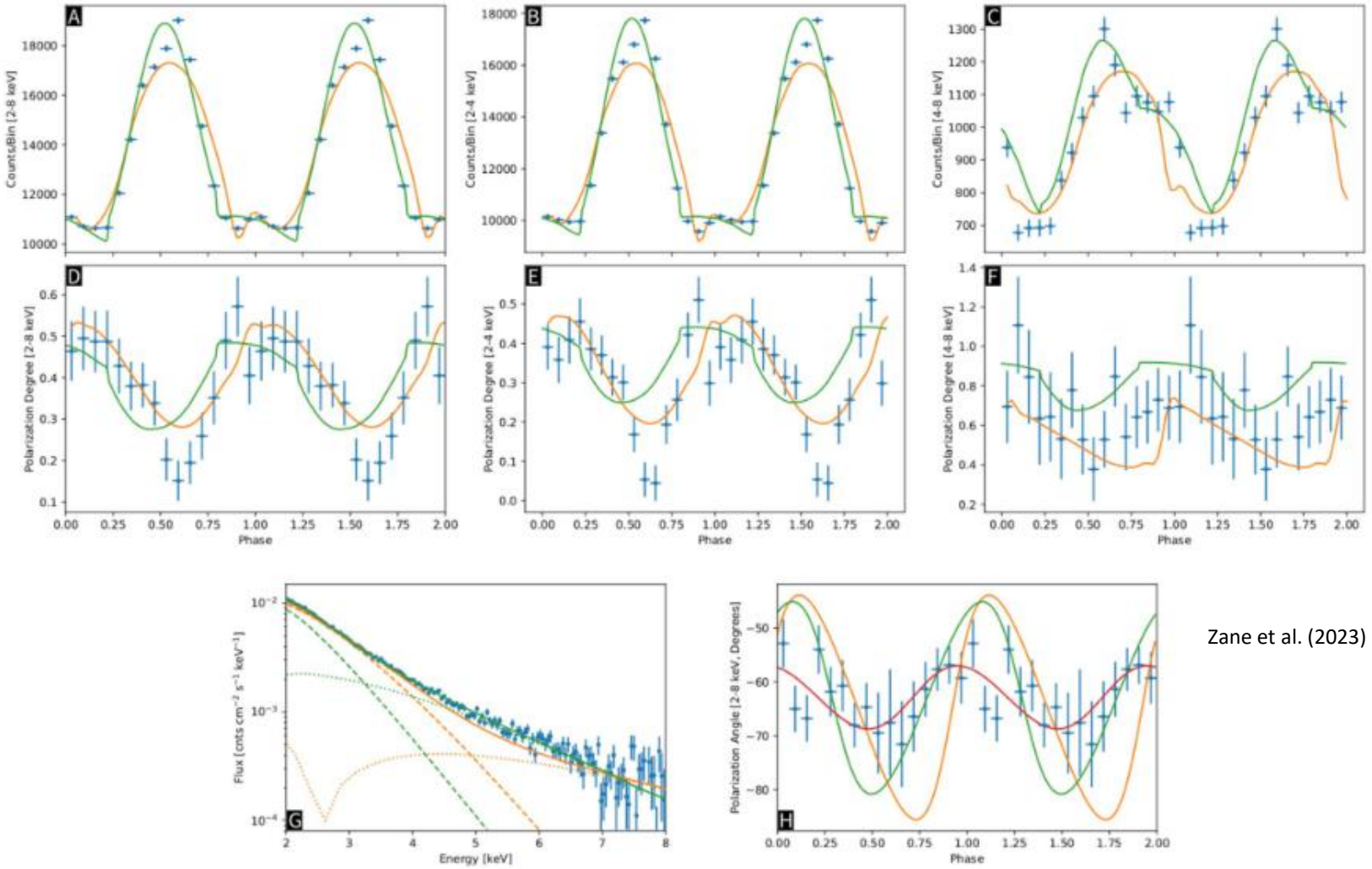

CAP+BELT model

2 CAPS model

Zane et al. (2023)

SGR 1806–20 – Theoretical interpretation

- Fitting the pulse profile with a condensed surface model + RCS (4U like) gives a energy-dependent PD not uncompatible with what IXPE found

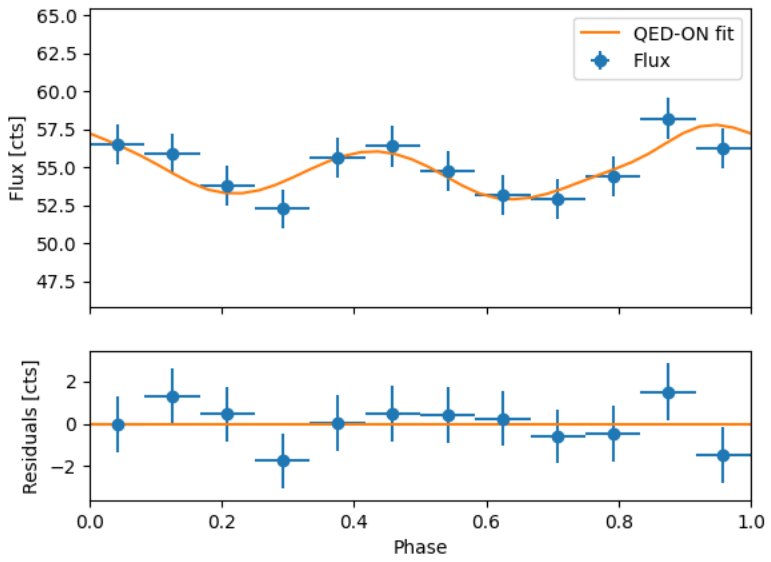

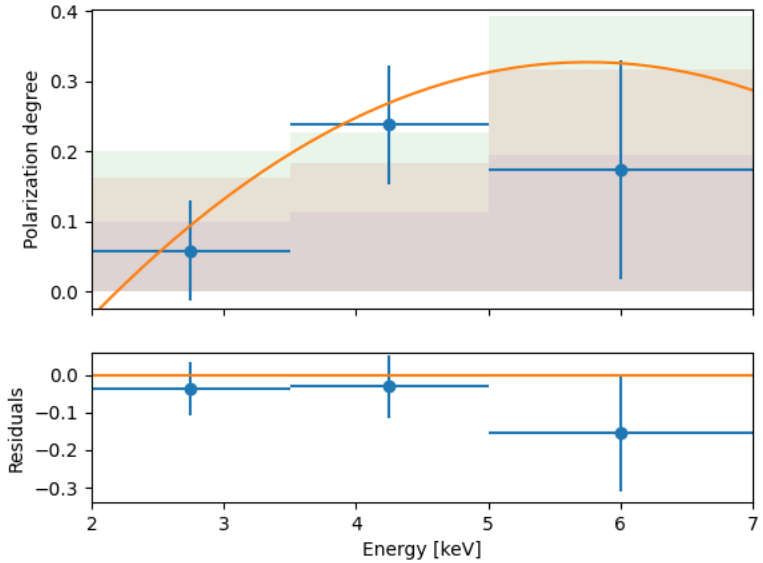

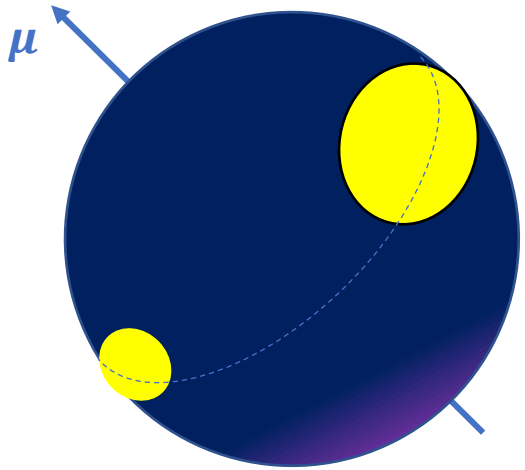

CS+RCS